Efficacy of Microbially Induced Calcite Precipitation in Carbonate Rich Soils

By

VALERIE ROSE YAÑEZ

THESIS

Submitted in partial satisfaction of the requirements for the degree of

MASTER OF SCIENCE

in

Civil and Environmental Engineering

in the

OFFICE OF GRADUATE STUDIES

of the

UNIVERSITY OF CALIFORNIA

DAVIS

Approved:

Jason T. DeJong, Chair

Douglas Nelson

Alejandro Martínez

Committee in Charge

2021

Efficacy of Microbially Induced Calcite Precipitation in Carbonate Rich Soils

ABSTRACT

There is a growing interest in microbially induced calcite precipitation (MICP) treatment in carbonate rich soils. Research has found MICP bio-augmentation and bio-stimulation to be effective in carbonate rich soils with potential differences dependent on chemical formulation, treatment time, soil composition and soil fabric. This study focused on lab-scale MICP stimulation applications on carbonate rich soils in preparation for large scale tests and field trials. This test program investigated the robustness of bio-stimulation in carbonate particles with respect to the effectiveness of treatment solution concentrations, the effectiveness of commercial grade chemicals, and the effectiveness of byproduct removal in carbonate rich soils. Despite significant differences in urea degradation between treatment solution concentrations, all soil columns resulted in improvement in shear wave velocity (V_s) and increase in calcite contents. Results showed commercial grade chemicals can be as effective as laboratory grade chemicals in bio-stimulation applications and ammonia byproduct removal methods decreased aqueous ammonia concentrations by four to five orders of magnitude. The results of this study suggest MICP bio-stimulation is successful for laboratory scale and may be successful in field scale applications.

ACKNOWLEDGEMENTS

I am grateful for all the mentorship and support I received throughout my undergraduate and graduate studies from the UC Davis Civil Engineering faculty. I would like to recognize my graduate advisor, Jason T. DeJong for his patience, motivation and guidance through my research and graduate studies. I would also like to recognize Colleen Bronner for her professional and personal support through my undergraduate and graduate career. I would like to acknowledge my thesis committee Professors Douglas Nelson and Alejandro Martinez for providing insightful feedback and guidance.

This work would not have been possible without the mentorship from Charles Graddy and Alexandra San Pablo. This dynamic duo taught me everything I know about MICP. I would also like to thank Professor Mike Gomez and Minyong Lee for their support and guidance in the research process and Shaivan Hirebelaguly Shivaprakash for assistance in post-treatment processing.

I am grateful for the support I received from my family, friends and cohort. Thank you to my family and friends for believing in me. Thank you to my cohort for fostering a welcoming environment and always pushing me to do my best.

The presented study involves work supported by the Engineering Research Center Program of the National Science Foundation under NSF Cooperative Agreement No. EEC-1449501. SEM and EDS at the University of California, Davis were made possible through the NSF-grant, MRI-1725618, used to purchase the ESEM. Any opinions, findings, and conclusions or recommendations expressed in this manuscript are those of the authors and do not necessarily reflect the views of the National Science Foundation.

TABLE OF CONTENTS

LIST OF FIGURES

1. INTRODUCTION

This research is part of a joint project between the Center for Bio-mediated and Bio-inspired Geotechnics (CBBG), Queen's University Belfast Energy Efficient Materials Research Center (EEM) and the Irish Center for Research in Applied Geoscience (iCRAG). The role of CBBG researchers is to support and collaborate on successful Microbially Induced Calcite Precipitation (MICP) treatment of Irish carbonate rich sand deposits in Blessington, Ireland. The UC Davis role includes establishing and optimizing the MICP treatment formula for the Blessington Sand. The objective of this study is to improve understanding of the robustness of bio-stimulation, the effectiveness of commercial grade chemicals, and the effectiveness of byproduct removal in carbonate rich soils.

Microbially induced calcite precipitation is a bio-cementation ground improvement method in which microbial activity is used to drive the precipitation of calcium carbonate at the contacts between soil particles to improve engineering properties. MICP has shown significant promise as a more sustainable alternative to traditional ground improvement methods in mitigating liquefaction (DeJong et al. 2006; Montoya et al. 2013; Burbank et al. 2013; Han et al. 2016; Feng and Montoya 2017; Xiao et al. 2018; Darby et al. 2019) and increasing soil shear strength and shear stiffness with small reductions in hydraulic conductivity (Montoya et al. 2013; Montoya and DeJong 2015; Gomez and DeJong 2017). Other traditional ground improvement methods have proved to be energy intensive processes and often require injection of hazardous chemical to improve soil properties (Raymond et al. 2020).

The common implementation methods for MICP are bio-augmentation and bio-stimulation of ureolytic bacteria. The bio-augmentation process requires injection of ureolytic bacteria such as *Sporosarcina pasteurii* into the soil to establish the necessary ureolytic activity. Bio-stimulation, however, enriches ureolytic bacteria naturally present in the soil to facilitate the cementation process (Fujita et al. 2008; Burbank et al. 2011; Gomez et al. 2014, 2016; Graddy et al. 2018, 2021). MICP treatments through bio-augmentation and bio-stimulation have been shown by other researchers to be effective in improving

the engineering properties of carbonate rich soils found commonly in near shore environments (Dyer and Viganotti 2017; Liu et al. 2018, 2019; Xiao et al. 2018, 2019; Fang et al. 2020; Lei et al. 2020; Li et al. 2020, 2021). Studies have tested soils ranging from 20% to 97% carbon content by mass. These studies have varied from small volume tests in syringe columns to field scale trials.

The small volume bio-augmentation and bio-stimulation tests have investigated the following treatment variables with respect to MICP treatment in soils with high carbonate contents; dissolution of in-situ calcite for carbonate precipitation (Liu et al. 2018; Casas et al. 2019), varying concentrations of yeast extract, urea and calcium chloride (Oualha et al. 2020; Wang et al. 2021), addition of fibers (Lin et al. 2019; Fang et al. 2020; Lei et al. 2020) and varying alkaline environments (Miftah et al. 2020; Oualha et al. 2020). Small volume studies have resulted in calcite precipitates forming at particle contacts (Dyer and Viganotti 2017; Xiao et al. 2018; Liu et al. 2018, 2019; Fang et al. 2020; Lei et al. 2020; Li et al. 2020, 2021), increase in compressive strengths from increase in cementation solutions (Liu et al. 2018; Xiao et al. 2018; Liu et al. 2019; Lei et al. 2020; Li et al. 2021), increasing interface shear resistance against steel (Li et al. 2020, 2021) and decreasing liquefaction potential (Xiao et al. 2018, 2019).

More specifically, Wang et al. (2020) compared yeast extract, malt extract, and nutrient broth as the enrichment media to determine which promoted the most ureolytic activity. These media were tested with urea concentrations ranging from 0 to 170 mM in continuously mixed 50 mL tubes containing 1g of soil to 50 mL of solution over a 72-hour period. The study used pH, electric conductivity, and urea degradation over the course of the experiment to evaluate ureolytic activity. Wang et al. (2020) found yeast extract and nutrient broth promoted the highest levels of ureolytic activity. While this study showed yeast extract is a preferable enrichment media for MICP application in carbonate rich sands, this small scale experiment does not provide insight into application on a column or field scale.

Many studies examined the mineralogy and morphologies of MICP treated carbonate sands via Scanning Electron Microscope (SEM) and X-ray Powder Diffraction (XRD)(Dyer and Viganotti 2017; Xiao et al. 2018; Liu et al. 2018, 2019; Fang et al. 2020; Lei et al. 2020; Li et al. 2020, 2021). Dyer and Viganotti (2017) specifically focused on comparing the formation of calcite precipitates in carbonate sands in comparison to silica sands. The small column tests in the experiment were treated using bio-augmentation and varied in timing and treatment retention. The study found more abundant and widespread precipitates in carbonate sand compared to silica sands, which was mainly attributed to the abiotic precipitation promoted by the in-situ carbonate component and increase in bacteria attachment to the rough carbonate particle surfaces. After cementation, both Dyer and Viganotti (2017) and Xiao et al. (2018) found it difficult to distinguish between carbonate precipitates and the carbonate sand particles. SEM images from Liu et al. (2018, 2019) and Li et al. (2020) showed carbonate precipitates coating particle surfaces. However, the methods in (Li et al. 2020) also showed formation of carbonate precipitates at particle contacts in the form of spherical and block crystals.

Many studies used unconfined compression strength (UCS) as a metric to show increase in soil strength as a result of MICP treatment. Studies conducted by Lin et al. (2019), Fang et al. (2020) and Lei et al. (2020) found UCS and calcite content to increase with an increase in fiber content. They showed fiber contents reduce the pore space between particles and preferential calcite precipitation occurred around fibers. Research conducted by Liu et al. (2018, 2019) and Miftah et al. (2020) attributed the increase in compressive strength to the increase in cementation volume applied and addition of treatment cycles.

Although a limited number of studies have examined field scale applications of MICP in carbonate sands, Oualha et al. (2020) was able to obtain an increase in calcite content of 16.2% in a field scale application through bioaugmentation using *B. cereus*. This trial showed the feasibility of MICP on a larger

scale, but it lacked details regarding the constituents and concentrations used for the cementation solutions to attain a 16.2% increase in calcite content.

A growing concern for MICP field application includes removal of ammonia byproducts. After completion of cementation treatments, ammonia is present both in solution and sorbed to soil particles. While the EPA does not currently have limits for ammonia concentrations in drinking water, there is concern from leaving high ammonia concentrations in the subsurface (U.S. Environmental Protection Agency 2013). Although there are a limited number of studies that have investigated the removal of ammonia, some studies have used injected "rinse" solutions for byproduct removal (van Paassen 2011; Cuthbert et al. 2013; Lee et al. 2019). Specifically, Lee et. al. (2019) investigated ammonia removal from a 3.7-meter MICP cemented soil column using a constant application of high pH and high ionic strength rinse solution. This study examined varying pore volumes of rinse solution required and varying detention time for rinsing solution (Lee et al. 2019).

In summary, prior work indicates that MICP can effectively improve carbonate rich soils with potential differences occurring dependent on chemical formulation, treatment time, soil composition, soil fabric, etc. This study aims to understand the robustness of MICP stimulation in lab scale applications in preparation for future large-scale tests and field trials in carbonate rich soils. Herein are reported the results from a test program on seven lab scale columns that were designed to investigate the impact of stimulation solution concentrations, grade of chemicals employed (commercial versus laboratory grade), treatment formulation chemical ratios, and soil composition on outcomes of bio-stimulated MICP treatments. In addition, the efficiency of ammonia byproduct removal in a carbonate rich soil was investigated.

2. METHODS & MATERIALS

2.1 Soil Materials

The two types of soil used to conduct this study were Blessington Sand(BS) and Concrete Sand(CS). The Blessington Sand was excavated from the Redbog quarry in Blessington, Ireland. It is noted that the samples received for testing were from a shallow excavation above the ground water table. The samples were obtained in Fall 2020 and stored at University College Dublin before shipment to UC Davis where they were homogenized with a cement mixer. These samples had a residual moisture content of 15%. No groundwater samples or analytical chemistry tests of the groundwater are available. Concrete Sand, a predominately silica sand typically used at UC Davis for MICP research (Gomez et al. 2016; Gomez and DeJong 2017; Lee et al. 2019; San Pablo et al. 2020), was quarried from an alluvial deposit in Woodland, California and had a residual moisture content of 2%. All samples were sealed for storage to maintain the natural moisture content.

The grain size distribution and soil properties are included for both sands in Table 1 and Figure 1. The Blessington Sand properties were consistent with (Igoe and Gavin 2019) with 26.5% fines, D_{60} = 0.16mm and D_{30} = 0.08 mm. Initial calcite content was determined to be 28.9%. The Blessington Sand was rounded and had higher sphericity with approximate values of 0.7 for roundness and 0.9 for sphericity (Mitchell and Soga 2005) The Concrete Sand had D_{60} = 1.7 mm and D_{10} = 0.25 mm and an initial calcite content of 0.1%. The Concrete Sand was angular and had low sphericity with approximate values of 0.5 for roundness and 0.3 for sphericity (Mitchell and Soga 2005).

Table 1: Summary of soil properties.

Soil Material	USCS	Source	Deposition	D_{10} (mm)	D_{30} (mm)	D_{60} (mm)	C_u	C_c	Fines Content (%)	Initial Carbonate Content (%)
Concrete Sand (CS)	SW	Woodland, Ca	Alluvial	0.25	0.70	1.70	6.8	1.15	0.9	0.1
Blessington Sand (BS)	SM	Blessington, Ireland	Lacustrine Delta	-	0.08	0.16	-	-	26.5	28.9

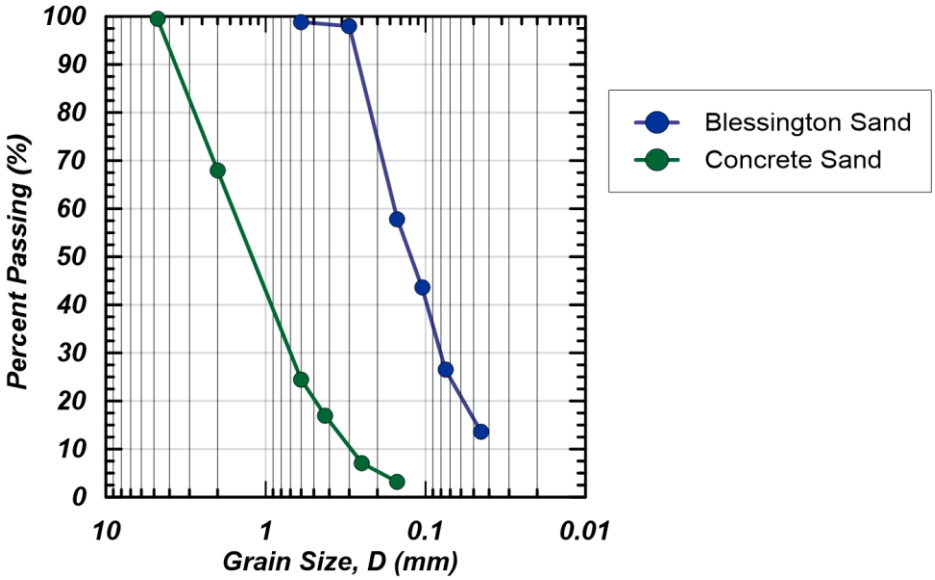

Figure 1: Grain size distribution for Blessington Sand and Concrete Sand.

2.2 Soil Columns

Seven cylindrical polytetrafluoroethylene (PTFE) soil columns (6.8 cm ID, 12 cm height) were configured with bender elements and one sampling port each at mid-height prior to soil placement. Bender elements were oriented horizontally with distances ranging from 53 to 63 mm tip to tip. All columns and tubing were autoclaved and all packing tools were wiped with Ethanol to minimize bacterial contamination from previous column experiments.

Blessington Sand and Concrete Sand were sequentially homogenized in a cement mixer for 15 minutes to ensure uniformity when packing columns. The cement mixer was power washed with water between homogenization of each soil type. Columns were packed in 3 lifts and tamped 15 times per lift to the target void ratio between 0.72 and 0.85. Ported PTFE caps were sealed with a nitrile o-ring and lined with Porex filters (125 – 195 μm) to prevent soil loss. Silicone caulking was applied externally to fittings to further prevent loss via leaks. An overburden pressure of 100 kPa was applied by spring force acting on the top cap to mimic a saturated depth of 10 meters as shown by the treatment schematic in Figure 2.

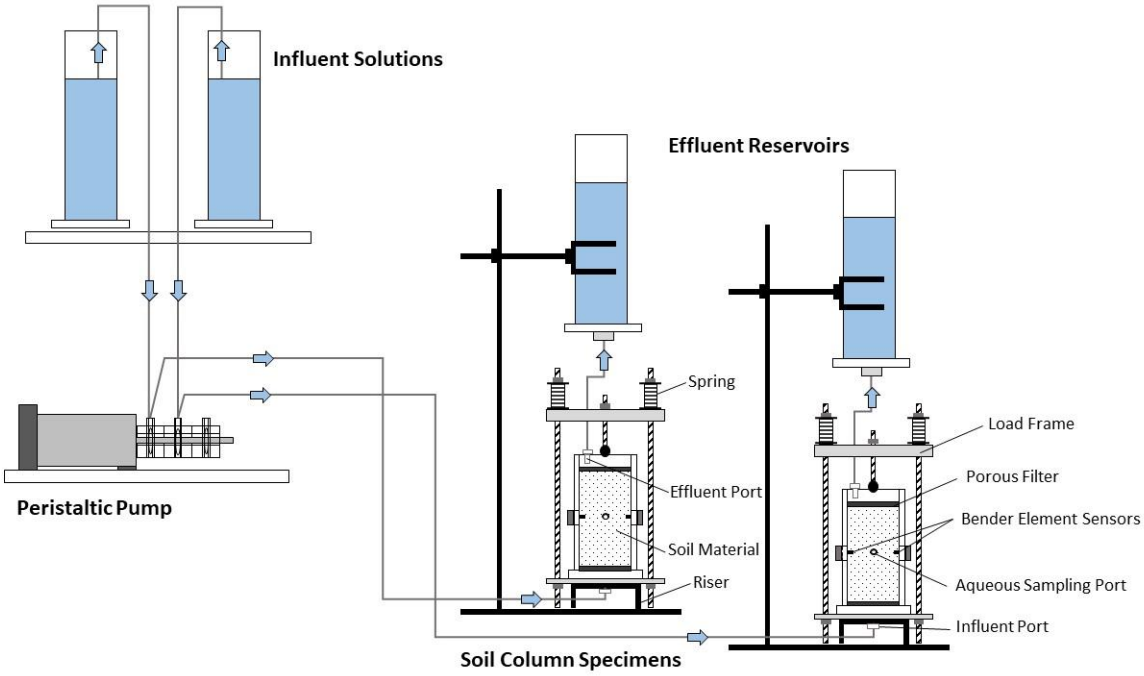

Figure 2: Schematic of columns detailing bottom upwards injection setup using peristaltic pumps, effluent collection with reservoirs and locations of sampling ports and bender elements.

2.3 Soil Column Test Matrix

The seven columns prepared for this experiment aimed to demonstrate feasibility of MICP stimulation in Blessington Sand while using Concrete Sand as the control (given the extensive prior results on this soil). These columns were established to compare the effects of varying yeast extract enrichment, slow/fast rates of stimulation, different urea to calcium ratios during cementation, commercial chemicals, and ammonia byproduct removal. The soil column matrix is summarized in Table 2.

Chemical concentrations for columns varied in yeast extract, urea and calcium concentrations to understand the effect of reducing chemical concentrations on sample cementation. Yeast extract concentrations of 0.02 g/L and 0.2 g/L were used to create slow and fast stimulation conditions. Previous experiments have found 0.02 g/L and 0.2 g/L to be effective in creating conditions where the bulk ureolytic rate for MICP stimulation can reduce 350 mM of urea in about 48 and 96 hours respectively (Gomez et al. 2018b; San Pablo et al. 2020).

Urea concentrations during stimulation varied between 50 and 350 mM because previous studies have shown a reduction in urea concentration from 350 to 50 mM does not have significant effect on stimulated bulk ureolytic rates (Gomez et al. 2018b). Columns receiving 350 mM of urea during stimulation received 1.4:1 or 350 mM to 250 mM urea to calcium concentrations during cementation treatments as used in previous experiments (Gomez et al. 2016, 2018b; San Pablo et al. 2020). Columns receiving 50 mM urea during stimulation received 1:1, or 250 mM to 250 mM, urea to calcium concentrations during cementation, as previous studies showed that reduction in urea concentrations during cementation achieved comparable cementation levels compared to the 1.4:1 ratios previously used (Gomez et al. 2016, 2018b; San Pablo et al. 2020).

The column labeling convention is defined by the soil type and chemical concentrations during the different phases of MICP. The names include soil type, yeast extract concentration in g/L, Urea concentration during stimulation in mM, ratio of urea to calcium chloride concentration during

cementation, and additional notation if commercial chemical were used (no addition if laboratory grade chemicals were used). For example, column BS_0.2_50_1:1_COM contained Blessington Sand, received 0.2 g/L of yeast extract used during the full experiment, 50 mM urea during stimulation, a 1:1 ratio of urea to calcium carbonate during cementation, and commercial grade chemicals were used.

Table 2: Soil test column matrix.

Column	Sand	Void Ratio	Yeast Extract [g/L] for All Treatments	Urea [mM] During Stimulation	Urea to Calcium Chloride [mM] During Cementation	Testing*
BS_0.02_50_1:1	Blessington Sand	0.86	0.02	50	250:250	UCS
BS_0.02_350_1.4:1	Blessington Sand	0.86	0.02	350	350:250	UCS
BS_0.2_50_1:1	Blessington Sand	0.83	0.2	50	250:250	Ammonia Sorption
BS_0.2_350_1.4:1	Blessington Sand	0.81	0.2	350	350:250	UCS
BS_0.2_50_1:1_COM	Blessington Sand	0.79	0.2	50	250:250	Rinsing
CS_0.2_50_1:1_COM	Concrete Sand	0.73	0.2	50	250:250	Rinsing
CS_0.2_50_1:1	Concrete Sand	0.72	0.2	50	250:250	Ammonia Sorption

* All columns processed for pH, urea, V_s, calcite content, LOI, TGA, SEM, and XRD.

2.4 Treatment Program

Soil columns were treated with 400 mL stimulation, flush, or cementation treatments dissolved in the artificial groundwater solutions specified in Table 3. Artificial ground water was composed of 0.04 mM potassium nitrate, 0.45 mM magnesium sulfate, 1.75 mM calcium chloride, 0.04 mM sodium nitrate, 1.10 mM sodium bicarbonate, and 0.06 mM potassium bicarbonate (Ferris et al. 2004). The treatment volume of 400 mL is the equivalent of 3 PV in the Blessington Sand and 2.5 PV in the Concrete Sand.

Figure 2 presents a schematic of the treatment set up where treatments were applied to columns using peristaltic pumps to deliver the full treatment volume in about 15 minutes to ensure constant pumping for both Blessington and Concrete Sand columns. Solutions were pumped bottom-up with a reservoir at the effluent to prevent desaturation of columns during fluid sampling. The effluent was discarded daily prior to the injection of each treatment.

Prior to stimulation (Day 0), columns were saturated with 800 mL of artificial ground water to saturate the soil columns. During the saturation process some fines were flushed out of the test specimens. Stimulation treatments were applied every 24 hours except for 48 hours between the first and second treatment (Gomez et al. 2018b; Lee et al. 2019). Stimulation solutions were pH adjusted to 9.0 as described by (Gomez et al. 2018b) for preferential selection of ureolytic microorganisms.

After 6 stimulation treatments, columns received a flush solution before the first cementation solution to prevent chemical precipitation inside the columns from the mixing of resident carbonate ions with influent calcium ions (Gomez et al. 2019). A total of 10 cementation treatments were applied once per 24 hours for all columns except for the slow stimulation columns (BS_0.02_50_1:1 and BS_0.02_350_1.4:1). These columns required 48 hours between cementation treatments in order for the injected urea to be mostly consumed. After the cementation phase all columns except the columns that received commercial chemicals were disassembled, extruded, and oven dried. Columns BS_0.2_50_1:1_COM and CS_0.2_50_1:1_COM received rinse solutions containing 200 mM potassium

chloride for ammonia removal. A total of approximately 12 PV were pumped in 1 PV increments each 24-hour period to remove most of the remaining ammonia.

Table 3: Summary of treatment solution chemical compositions.

Constituent	**Treatment**			
	Stimulation	***Flush***	***Cementation***	***Rinse***
Urea (mM)	50 or 350	-	250 or 350	-
Ammonium chloride (mM)	100	12.5	12.5	-
Sodium acetate trihydrate (mM)	42.5	42.5	42.5	-
Yeast extract (g/L)	0.02 or 0.2	0.02 or 0.2	0.02 or 0.2	-
Calcium chloride (mM)	-	-	250	-
Potassium Chloride (mM)	-	-	-	200
pH	9.0*	~	-	9.0**

*pH adjusted with 2.0-2.5 mL of 5 M NaOH.
**pH adjusted with 75 µL of 1 M NaOH.

3. TREATMENT & MONITORING MEASUREMENTS

3.1 Aqueous Sampling

Aqueous samples were collected to monitor changes in solution pH, urea, and ammonia concentrations. Samples were collected in two 2 mL samples daily before and after pumping of the treatment solution via needle and syringe from mid-height sampling ports. An additional 2 mL were sampled for urea time course mapping during stimulations 2, 4 and 6 as well as during cementations 2, 6 and 10. Time course samples were collected 1, 2, 4 and 8 hours after treatment injection for the fast stimulation columns and 4, 8, 24 and 32 hours after treatment for the slow stimulation columns. Samples for pH were measured and then frozen at -20°C. Samples for urea and ammonia were frozen immediately for later analysis.

Samples taken for urea were used to measure concentrations in triplicates using a colorimetric reagent similar to (Knorst et al. 1997). Samples were diluted with a mixture of 4% weight to volume of p-dimethlyaminobenzaldehyde, 4% volume to volume 12 M hydrochloric acid and absolute ethanol. Sample absorbance were conducted at 422 nm using a spectrophotometer.

Samples for ammonia were collected in 2 mL tubes before and after each injection of the potassium chloride rinse from the sampling port at mid-height. An additional 2 mL were sampled from the homogenized effluent solution. Total NH_4^+ measurements were completed using a salicylate reaction method similar to (Krom 1980; Lee et al. 2019). Two reagents were used to dilute samples and then measure absorbance values with a micro plate spectrophotometer at 650 nm. The first reagent contained (weight/volume) 0.05% sodium nitroprusside, 13% sodium salicylate, 10% sodium citrate, and 10% sodium tartrate in water in weight per volume. The second reagent contained 5% sodium hypochlorite (volume/volume) and 6% sodium hydroxide (weight/volume) in water.

3.2 Shear Wave Velocity

Shear wave velocity (V_s) measurements were taken using bender element pairs at mid-height of each column and were oriented horizontally. Shear waves were propagated horizontally and polarized in the vertical direction. Bender elements were fabricated and waterproofed with epoxy, electronics wax, and an insulation coating (Chaney et al. 1996; Gomez et al. 2016; Lee and Santamarina 2005; Montoya et al. 2012). A 24V 100 Hz square wave was transmitted and signals were received by the bender element pair using an oscilloscope with a sampling frequency of 1 MHz. V_s measurements were taken daily before treatment solutions. These measurements were visually interpreted based on the arrival time at the first peak of the shear wave and measured sensor spacings. Measurements were filtered using a Python 3.7 script with a 30,000 Hz high frequency corner and 200 Hz low frequency corner.

3.3 Strength

Soil columns were extruded using a hydraulic jack while ensuring not to exceed 3,500 kPa to limit sample disturbance. Extruded samples were then oven dried at 60°C for at least 72 hours in preparation for unconfined compressive strength testing. Columns BS_0.02_50_1:1, BS_0.02_350_1.4:1 and BS_0.2_350_1.4:1 were tested at 1% strain per minute until failure using a Geo-Tac apparatus.

3.4 Soil NH_4^+ Measurements

Soil columns BS_0.2_50_1:1, CS_0.2_50_1:1, BS_0.2_50_1:1_COM, and CS_0.2_50_1:1_COM were separated into top, middle and bottom sections after extrusion and frozen at -20°C with residual moisture for later extraction to quantify the NH_4^+ concentration remaining sorbed on the soil particle surface. Columns BS_0.2_50_1:1 and CS_0.2_50_1:1 were used to represent sorbed ammonia concentrations without rinsing, and BS_0.2_50_1:1_COM and CS_0.2_50_1:1_COM samples were used to represent sorbed ammonia concentrations after KCl rinse applications.

Sorbed ammonia quantification followed similar method outlined by Lee. et. al. (2019). Moist soil samples were thawed and homogenized, and then sample water contents and mass were obtained. Approximately 30 grams of moist soil sample were filtered with a with 0.45 micron nylon filter baskets and centrifuged at 3800 rpm for 1 hour to extract solutions. Approximately 2 mL of solution was collected and analyzed for aqueous NH_4^+ concentrations. Sorbed NH_4^+ concentrations were measured using the KCl extraction process outlined by Keeney and Nelson (1982). A 20 mL solution of a 2 M KCl was mixed with 10 grams of the centrifuged soil and allowed to equilibrate to remove NH_4^+ ions from soil particle surface. Then 2 mL of the solution was collected and measured for NH_4^+ concentrations. Sorbed NH_4^+ masses were determined by subtracting the NH_4^+ masses from free solution by the NH_4^+ measurements after the KCl extraction.

3.5 Calcite Conetent

Columns were divided into thirds; a top, middle and bottom section for carbonate content measurements. Samples were stored in an oven at 60°C to prevent carbonate dissolution or remineralization. Carbonate contents were measured by mass following ASTM D4373-14 (ASTM International 2014). Oven dried samples were mixed with 2 M hydrochloric acid in a sealed pressure chamber where carbonate dissolution produces carbon dioxide gas. The increase in pressure was measured once the hydrochloric acid and soil sample were stable. The results were converted using developed calibration relationships to determine carbonate content. Calcite contents were then measured for the untreated in-situ soils and in triplicates for each section of MICP treated columns.

3.6 Total Carbon

Soil samples were processed through various combustion methods to determine initial and final carbon contents to convert to calcite contents. Samples processed ranged from 50 to 100 g of soil from

the middle section of each column and from untreated soil samples. Soil samples were processed using loss-on-ignition (LOI) and thermogravimetry analysis (TGA).

LOI was determined by heating samples in a muffle furnace according to ASTM D7348 (ASTM International 2013)**,** Method B (combustion at 950 °C) (Wirth et al. 2019b; a). Samples were combusted at 950°C for 2 hours using a Nabertherm P300 oven.

TGA was conducted using a Hitachi TG/DTA 7300 device. Samples were heated to 150 °C at a rate of 20°C/minute, held steady for 5 minutes and then heated to 950 °C at a rate of 25°C/minute in a nitrogen atmosphere (flow rate of 100 cc/min). The atmosphere was then changed to compressed air to allow for combustion of free carbon phases (Wirth et al. 2019b; a). All LOI and TGA soil samples were processed in Professor Susan Burn's laboratory at the Georgia Institute of Technology.

3.7 Permeability

Columns were tested for final permeability using falling head tests. The falling head test was conducted on day of the 10^{th} cementation treatment application using the cementation solution to not introduce additional chemicals. Permeability measurements were recorded for columns BS_0.2_50_1:1_COM and CS_0.2_50_1:1_COM during the final rinse treatment of the potassium chloride rinse solution.

3.8 SEM, XRD and EDS

Soil samples were processed using SEM and XRD by Professor Susan Burn's laboratory at Georgia Institute of Technology. Addition SEM and EDS scans were conducted by Andrew Thorn in the Advanced Materials Characterization and Testing laboratory at the University of California, Davis. Samples were oven dried for at least a 72-hour period and stored in individual airtight containers until they were scanned. Samples tested came from the middle section of all columns and untreated soil samples.

SEM images from Georgia Institute of Technology were obtained using a Thermo Scientific Phenom XL G2 Desktop SEM (used for untreated samples) and a Hitachi SU8010 Ultra-High Resolution (1.0nm) FE-SEM (for treated samples). Imaging was conducted at magnifications from 90x to 1,000x. XRD analyses conducted at Georgia Institute of Technology were completed using a Panalytical X'pert Pro Alpha-1.

The SEM's conducted at the University of California, Davis were completed using a ThermoFisher Scientific Quattro-S Environmental (E)SEM equipped with a Bruker XFlash Energy Dispersive X-Ray Spectrometer. The SEM was operated under low-vacuum, at a partial pressure of 150 Pa. The gas species used for low-vacuum operation was water. The Energy Dispersive X-Ray Spectra (or EDS) were obtained with an accelerating voltage of 30 kV used to acquire the images.

4. RESULTS & DISCUSSION

4.1 pH

The changes in pH during the experiment are presented in Figure 3 A-F. Figure 3A presents BS_0.02_50_1:1 and BS_0.02_350_1.4:1, Figure 3B presents BS_0.2_50_1:1 and BS_0.2_350_1.4:1, Figure 3C presents BS_0.2_50_1:1 and BS_0.2_50_1:1_COM, and Figure 3D presents CS_0.2_50_1:1 and CS_0.2_50_1:1_COM. Initial pH ranged from 7 to 8 for all columns which converged to a pH of 9.3 during stimulation except for column BS_0.02_50_1:1 in Figure 3A. Stimulation treatments were pH adjusted to 9.0 using sodium hydroxide to create a more alkaline environment for the ureloytic bacteria (Gomez et al. 2018b). Measurement of pH around 9.2 to 9.3 at the end of stimulation commonly signifies high ureolytic activity (Stocks-Fischer et al. 1999) which all columns except column BS_0.02_50_1:1 were able to achieve by the end of stimulation treatments. By the end of cementation, columns reached steady state at a pH of 8.0 for low ureolytic rate stimulation columns and 8.5 to 9.0 for high ureolytic rate stimulation columns.

From Figure 3B, column BS_0.2_50_1:1 achieved a pH of 9.3 after the second stimulation treatment and remained in steady state for the remainder of the stimulation phase, signifying full urea degradation for the remainder of the stimulation phase. Since the bulk ureolytic activity was established during stimulation, column BS_0.2_50_1:1 consistently reached a pH of 8.0 to 8.2 during cementation, signifying full urea degradation and consumption of the available calcium, for precipitation. While the trends in pH for column BS_0.2_50_1:1 signify ureolytic activity in Blessington Sand, column CS_0.2_50_1:1 in Figure 3D followed similar trends reaching steady state pH of 9.2 during stimulation and 8.0 to 8.2 during cementation signifying establishment of ureolytic activity in Concrete Sands. The fluctuations in pH over the 24-hour retention period reflect the ability of both columns to consume daily concentrations of calcium despite lower initial pH of 7.5 to 7.7 in column CS_0.2_50_1:1, which may be attributed to differences in soil minerology.

Since columns BS_0.2_50_1:1 and CS_0.2_50_1:1 were able to successfully stimulate ureolytic activity given the low urea concentrations used, the trends in pH for column BS_0.2_350_1.4:1 in Figure 3B, where the urea concentration was higher, are as expected. Column BS_0.2_350_1.4:1 reached a pH of 9.3 after the second stimulation treatment and a pH of 8.5 for the course of cementation treatments, reflecting steady state and full urea degradation in each treatment. The offset during cementation for initial and final pH for each treatment is reflective of the 1.4:1 urea to calcium chloride concentrations used. During cementation, the pH increases once the calcium is consumed at a 1:1 ratio with urea, then the degradation of the remaining 100 mM of urea continues to increase the pH. This is seen in the steady pH of 8 to 8.2 in columns BS_0.2_50_1:1 and CS_0.2_50_1:1 compared to the pH of 8.5 in column BS_0.2_350_1.4:1.

For the slow stimulation columns BS_0.02_50_1:1 and BS_0.02_350_1.4:1 in Figure 3A, 6 stimulation treatments were sufficient for column BS_0.02_350_1.4:1 given the low yeast extract concentration. However, the 6 stimulation treatments were not sufficient for column BS_0.02_50_1:1 as the column did not reach a pH above 9.1, signifying that it was unable to degrade the available urea. The column continued to stimulate progressively more during the first half of the cementation treatments, as it was not able to reach an increase in pH above 7.5 until the 5^{th} treatment. The lack of increase in pH during the first half of stimulation signifies the 50 mM of urea available were not fully degraded despite 48-hour retention times between treatments. Although the urea was not fully degraded there was concurrent calcium precipitation. Column BS_0.02_350_1.4:1 served as a lower bound practical limit of yeast extract concentrations that can achieve full urea degradation during the 6 stimulation treatments.

Columns BS_0.2_50_1:1 and BS_0.2_50_1:1_COM for Blessington Sand in Figure 3C and CS_0.2_50_1:1_COM and CS_0.2_50_1:1 for Concrete Sand in Figure 3D served as comparisons between laboratory and commercial grade chemicals. The Blessington Sand columns were able to reach a pH above 9.2 by the 5^{th} stimulation treatment and a pH above 8 for steady state conditions for all 10 cementation

treatments. Similarly, the Concrete Sand columns reached a pH above 9.2 by the 5th cementation treatment and pH above 8 for all cementation treatments. For both soils, the commercial grade chemicals were able to achieve comparable trends in pH to their laboratory grade counterparts signifying that despite impurities in the commercial grade chemicals they were still able to achieve bulk ureolytic activity. The two columns show comparable pH trends to those for the laboratory grade chemicals, indicating that industry chemicals could be used effectively in upscaled applications.

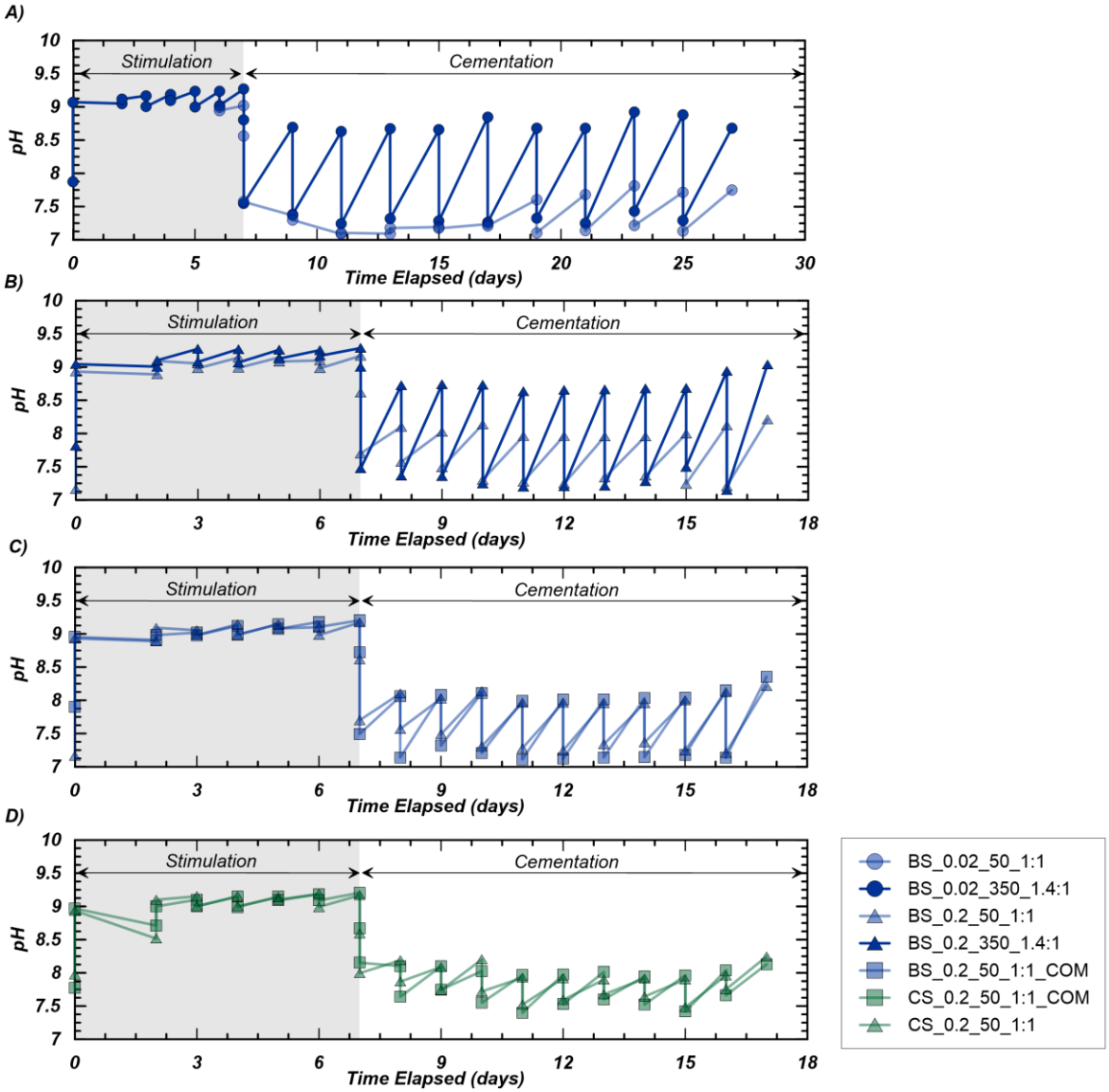

Figure 3: Measurements of pH at mid-height before and after pumping of each treatment for (A) BS_0.02_50_1:1 and BS_0.02_350_1.4:1, (B) BS_0.2_50_1:1 and BS_0.2_350_1.4:1, (C) BS_0.2_50_1:1 and BS_0.2_50_1:1_COM, and (D) CS_0.2_50_1:1 and CS_0.2_50_1:1_COM.

4.2 Urea – Initial and Final Concentration for Each Treatment

Figure 4 A-D present urea concentrations during stimulation and cementation treatments. This reflects sample concentrations taken immediately after solution injection, which should reflect the input concentration of urea for the stimulation or cementation solution, as well as urea concentrations in samples taken 24 hours after solution injection (immediately prior to next treatment) to understand the rate of urea hydrolysis during each treatment.

Both baseline conditions, column BS_0.2_50_1:1 and column CS_0.2_50_1:1 in Figure 4B and Figure 4D, respectively, reached full urea degradation before the end of the stimulation phase. Column BS_0.2_50_1:1 reached full degradation by the end of the 4th stimulation treatment and column CS_0.2_50_1:1 reached full degradation by the 3rd stimulation. Once both columns reached 100% urea degradation during stimulation of 50 mM, sufficient ureolytic activity was established to degrade the increase in concentration of 250 mM during cementation cycles.

There was a significant lag in establishing ureolytic activity in column BS_0.02_50_1:1 and column BS_0.02_350_1.4:1 based on the decrease in initial yeast extract conditions (shown in Figure 4A). The low yeast extract and low urea concentrations during the stimulation of column BS_0.02_50_1:1 slowed development of ureolytic activity. When the urea concentration during cementation was increased to 250 mM and the residence time was increased from 24 hours during stimulation to 48 hours during cementation, the gradual increase in urea degradation during the first 5 treatments is evident until urea was fully degraded during the 6th cementation cycle. Column BS_0.02_350_1.4:1, which had higher urea concentration during stimulation, did not reach full degradation during the 6 stimulation treatments. However, column BS_0.02_350_1.4:1 reached 90% degradation during the first cementation cycle and fully degraded the urea for the remainder of the experiment. The lag in degradation for both columns reflects that the 0.02 mg/L of yeast extract for the 6 stimulation cycles inhibited the column from

establishing sufficient ureolytic activity to yield the maximum precipitation benefits for MICP. If patterns observed in urea degradation during cementation held true for hypothetical additional stimulation treatments, column BS_0.02_50_1:1 would need 6 addition stimulation cycles and column BS_0.02_350_1.4:1 would need one more cycle to achieve full degradation during stimulation.

Comparisons between laboratory and commercial grade chemicals are shown in Figure 4C for Blessington Sand and Figure 4D for Concrete Sand. Both column BS_0.2_50_1:1 and CS_0.2_50_1:1_COM fully degraded initial urea concentrations by the end of the 3rd stimulation and remained steady for the remainder of the experiment. Column CS_0.2_50_1:1_COM and CS_0.2_50_1:1 fully degraded urea by the end of the 2nd stimulation and remained steady. Before and after measurements show laboratory and commercial grade chemicals for both soils were comparable in establishing ureolytic conditions but time course samples may provide further insight into bulk ureolytic rates.

In summary, 0.02 g/L YE was not sufficient to establish ureolytic activity during the 6 stimulation treatments but all columns with 0.2 g/L YE were able to establish desired bacteria communities within the 6 stimulation treatments. Both Concrete Sand columns reached full degradation by the 2nd stimulation while the Blessington Sand columns needed until the end of the 3rd cementation treatment to reach full degradation. Although these formulations were developed for application in Concrete Sand, the Blessington Sand only needed an extra treatment to be as robust and it did not inhibit performance in degradation during cementation. The failure of newly introduced urea to occasionally reach anticipated concentrations (e.g. day 15, Fig. 4B) likely reflects imperfect mixing.

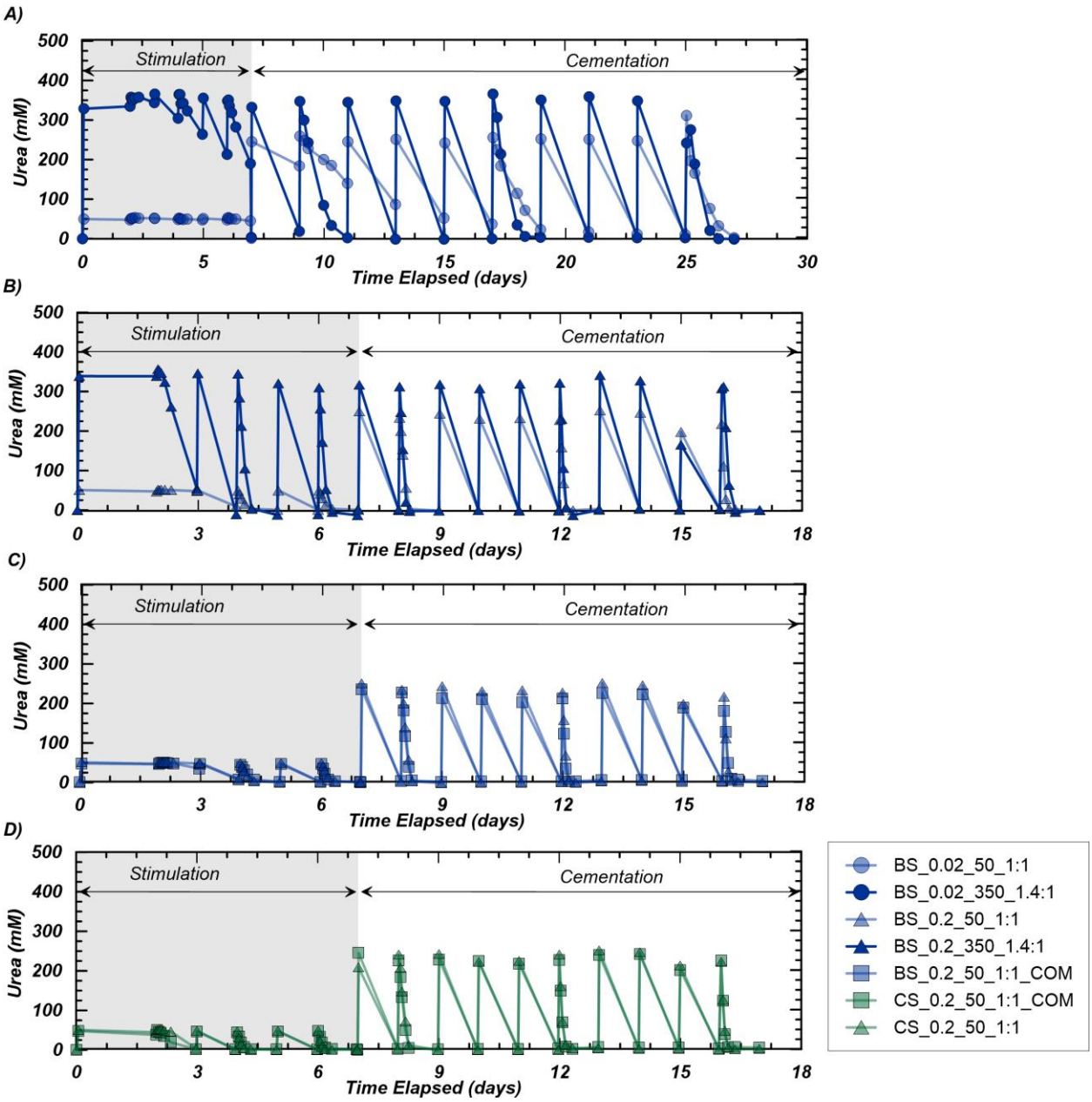

Figure 4: Concentrations of aqueous urea before and after pumping for each treatment for (A) BS_0.02_50_1:1 and BS_0.02_350_1.4:1, (B) BS_0.2_50_1:1 and BS_0.2_350_1.4:1, (C) BS_0.2_50_1:1 and BS_0.2_50_1:1_COM, and (D) CS_0.2_50_1:1 and CS_0.2_50_1:1_COM.

4.3 Urea – Concentration Changes Over Treatment Interval

Urea degradation during the time course sampling is shown in Figure 5 A-F. These results reflect the rate of urea degradation during the following treatments; stimulation 2, stimulation 4, stimulation 6, cementation 2, cementation 6 and cementation 10. Figures 5 A-C include urea degradation for all columns, Figures 5 D-F include urea degradation for high yeast extract columns and Figures 5 G-I include urea degradation for low yeast extract columns.

As seen in Figure 5, column BS_0.2_50_1:1 reached full urea degradation by the 2nd stimulation treatment and continued in steady state for the remainder of the treatment cycles. The time course shows full degradation required the 24 hour retention period during stimulation 2, but as ureolytic activity increased this column reached full degradation within 8 hours in stimulations 4 and 6 and within 4 hours during cementations 2 and 6. Column CS_0.2_50_1:1 showed similar results during stimulation 2; however, the low urea concentration introduced during stimulation was degraded within 4 hours for stimulation and the high urea concentration during cementation degraded within 8 hours for cementation 2 and 6 before achieving full degradation within 4 hours during cementation 10. Despite higher urea concentrations in column BS_0.2_350_1.4:1, the degradation rates during the cementation time courses fell slightly relative to the column BS_0.2_50_1:1 rates.

The low yeast extract columns showed an increase in degradation rates once the ureolytic activity was established. As shown in Figure 5, the activity in column BS_0.02_50_1:1 did not reflect degradation until cementation 2. Following cementation 2, the degradation rates showed a more significant increase with each cementation treatment. Despite little degradation during stimulation 2 for column BS_0.02_350_1.4:1, degradation rates increased in later stimulation treatments and there was a significant increase in activity reflected by the degradation in cementation treatments.

As shown in Figure 5, the Blessington Sand columns BS_0.2_50_1:1 and BS_0.2_50_1:1_COM followed similar degradation rates throughout the experiment. They did not fully degrade the 50 mM urea during stimulation 2, but it was degraded at an increasing rate within 8 hours in stimulation 4 and 6. With the increase in urea concentration during cementation, column BS_0.2_50_1:1, and BS_0.2_50_1:1_COM continued to fully degrade the urea within 8 hours from cementation 2 and 4 until the rates increased and reach full degradation within 4 hours for the final cementation treatment. The Concrete Sand columns CS_0.2_50_1:1_COM and CS_0.2_50_1:1 followed similar trends to the Blessington Sand columns, however they were able to fully degrade the input urea concentrations during the 24 hour retention period of stimulation 2 and then within an 8 hour period in stimulation 4 and 6. Both columns continued to fully degrade the urea within 8 hours for cementation 2 and 4 despite the increase in concentration. By cementation 10 urea was fully degraded within the first 4 hours.

Overall, urea degradation rates for all columns increased with additional stimulation treatments. Despite an increase in concentrations from 50 mM of urea during stimulation to 250 mM during cementation, degradation rates continued to increase with additional treatments. The degradation rate during cementation 2, 6 and 10 showed convergence despite varying chemical concentrations and soil type in all columns with 0.2 g/L yeast extract. This reflects the ability to establish sufficient ureolytic activity in Blessington Sand to establish favorable conditions for MICP. Also, the 50 mM concentrations of urea during stimulation proved to establish sufficient microbial activity in preparation for higher concentrations during cementation. This would allow for lower urea concentrations during larger trails to reach similar degrees of soil strength improvement. Both Concrete and Blessington Sand columns, commercial chemicals proved to reach the same degradation rates as laboratory scale chemicals.

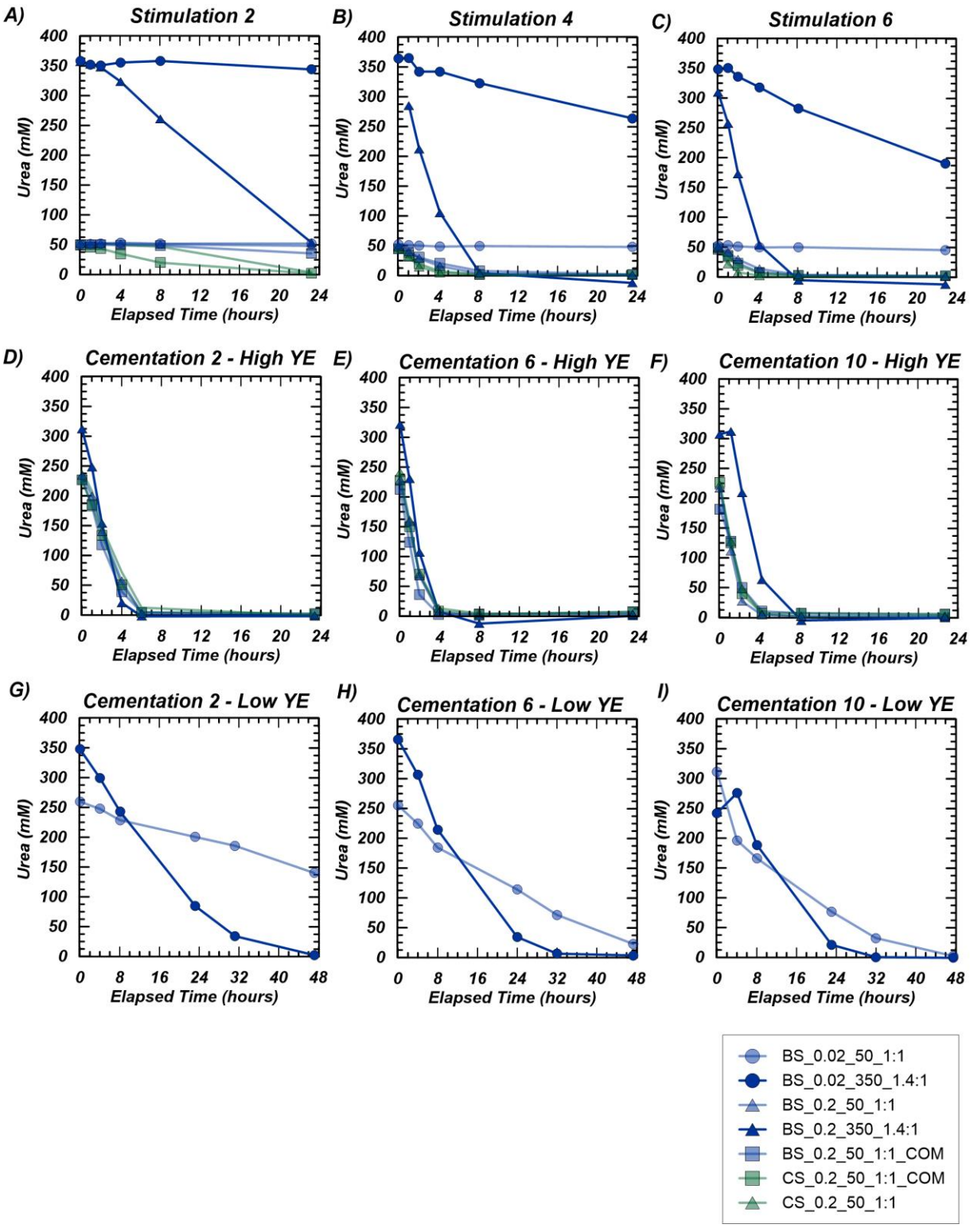

Figure 5: Concentrations of aqueous urea during time course sampling during (A) Simulation 2, (B) Simulation 4, (C) Simulation 6, (D) Cementation 2 – High YE, (E) Cementation 6 – High YE, (F) Cementation 10 – High YE, (G) Cementation 2 – Low YE, (H) Cementation

4.4 Urea – Zero and First Order Kinetics

Initial ureolysis rates were estimated from urea time course measurements during treatment retention periods for stimulation and cementation. Figure 6 presents the exponential (first-order kinetics) and linear (zeroth-order kinetics) estimations for urea concentration decrease per treatment. Figure 6A and Figure 6B present the measured urea concentrations for column BS_0.2_50_1:1_COM and CS_0.2_50_1.1_COM during stimulation 6 and cementation 10 superimposed by the first-order linear fit, and Figure 6D and Figure 6E presents their measured urea concentrations superimposed by the zeroth-order exponential fit for the degradation rates. Figure 6C presents the initial ureolysis rates for the first-order fit and Figure 6F presents the rates for the zeroth-order fit for the course of stimulation and cementation treatments for all columns.

As evident in column BS_0.2_50_1:1_COM and CS_0.2_50_1:1_COM the linear fit accurately captures the urea degradation within the first 3 to 4 hours after treatment application. For column BS_0.2_50_1:1_COM and CS_0.2_50_1:1_COM the linear trend reflects approximately 60% urea degradation for 50 mM during stimulation 6 and 80% during cementation 10. This trend is consistent in the remaining columns where the linear fit appropriately estimates the degradation rates in the first 4 hours of treatment retention. Zeroth-order ureolysis rates (Panel F) show the largest increase in ureolysis rates between treatment 6 to 12 (stimulation 6 to cementation 10). Low YE columns BS_0.02_50_1:1 and BS_0.02_350_1.4:1 reflected the lowest ureolysis rates which is consistent with pH and shear wave velocity trends as these columns continued to stimulate during cementation treatment because sufficient ureolytic activity was not established during the 6 stimulation treatments. Both columns reached a maximum of 20 mM/hr degradation by cementation 10. The commercial grade chemical columns and laboratory grade chemical columns followed similar trends with a slow increase in ureolysis rates of 0 to 20 mM/hr during stimulation treatments and then up to 80 mM/hr by cementation 6. Column

BS_0.2_350_1.4:1 with the highest chemical concentration achieved the highest ureolysis rate of 115 mM/hr during cementation 6.

The raw data and exponential fits in Figure 6D and Figure 6E were fit using the least squares method. The first-order ureolysis rates for columns with high YE extract concentrations (Panel C) reached 0.2 to 0.4 hr^{-1} except for column CS_0.2_50_1:1 which reached 0.8 hr^{-1}. Degradation continued to increase and reach 0.6 to 0.7 hr^{-1} by the end of cementation 10 expect for columns BS_0.2_350_1.4:1 and BS_0.2_50_1:1_COM which peaked during stimulation 6 and decreased to 0.3 and 0.5 hr^{-1}, respectively. The low YE columns reflected very little increase in ureolysis rates reaching a maximum of 0.05 hr-^{1} by the final cementation treatment. Overall, zeroth-order and first-order ureolysis rates highlighted the slow increase in urea degradation for the low YE columns. All columns with high YE concentration reached comparable linear an exponential degradation rates between both Blessington Sand and Concrete Sand.

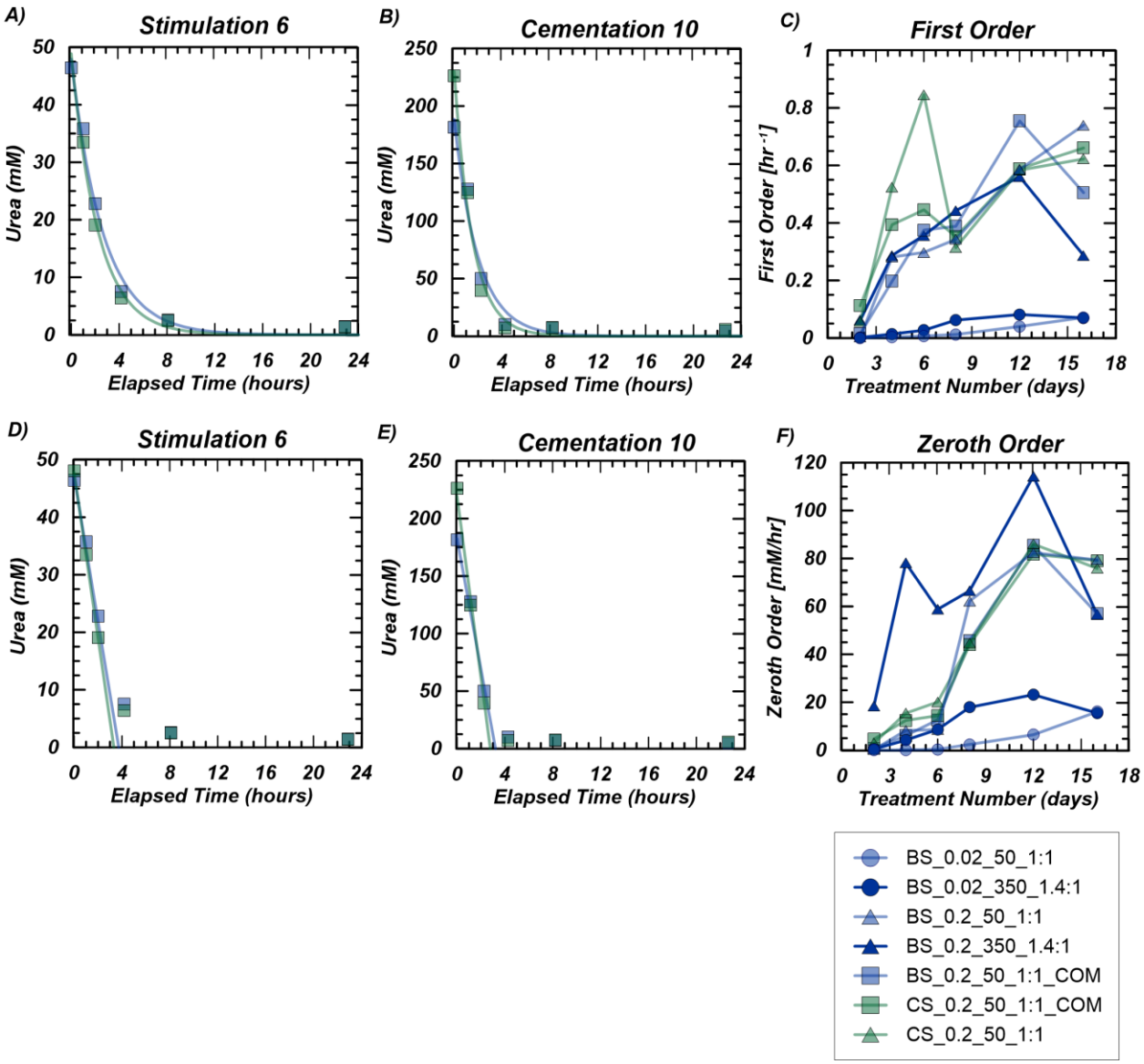

Figure 6: Kinetic modeling of initial ureolytic rate using Michaelis-Menten model with (C) first-order fitting to the initial pseudolinear portion and (F) zero-order exponential fitting using the measured data from BS_0.2_50_1:1_COM and CS_0.2_50_1:1_COM during (A & D) Stimulation 6 and (B & E) Cementation 10.

4.5 Ammonia and Desorption

Figure 7 presents the aqueous and sorbed ammonia concentrations for rinsing treatments. The aqueous ammonia concentration samples before and after injection of each potassium chloride rinse treatment for columns BS_0.2_50_1:1_COM and CS_0.2_50_1:1_COM as a function of rinse treatment and number of pore volumes are presented in Figure 7A and Figure 7B, respectively. Rinse treatments decrease the aqueous ammonia concentrations from 455 mM to 0.03 mM for BS_0.2_50_1:1_COM and from 468 mM to 0.09 mM in CS_0.2_50_1:1_COM.

Figure 7B presents the data as a function of the number of pore volumes of potassium chloride pumped. The pore volume is estimated to be 130 mL for BS columns and 160 mL for CS columns. After the 12 treatments BS_0.2_50_1:1_COM received approximately 12.6 PV of rinse solution and CS_0.2_50_1:1_COM received approximately 10.6 PV. By looking at the data in terms of PV, the ammonia concentrations decrease in magnitude at approximately the same rate where concentrations have decreased by 4 magnitudes by the 10^{th} PV.

Figure 7C and 7D present that data from Figure 7A and 7B in mmol of cumulative ammonia removed and percent removal respectively. Figure 7C shows the cumulative ammonia removal with respect to the total aqueous ammonia removed. Figure 7D shows the percent ammonia removed as a function of the total ammonia determined from the unrinsed columns BS_0.2_50_1:1 and CS_0.2_50_1:1 for aqueous and sorbed concentrations. Both figures show the largest removal in ammonia occurred within the 4 rinse treatments and then removal concentration decreased in orders of magnitude since removal after the 4^{th} treatment was equal or less than 1 mM per rinse treatment.

Figure 7E and 7F present the ammonia concentrations collected from the unrinsed columns BS_0.2_50_1:1 and CS_0.2_50_1:1. The unrinsed columns serve as pseudo replicates for the ammonia concentrations of BS_0.2_50_1:1_COM and CS_0.2_50_1:1_COM if they had been disassembled at the

end of cementation and not received rinse treatments. Figure 7E shows the aqueous concentration of moist soil sample taken from the unrinsed BS_0.2_50_1:1 to be 442 mM and the unrinsed CS_0.2_50_1:1 to be 518 mM. Figure 7F includes the sorbed ammonia concentration for unrinsed columns. The unrinsed BS had a sorbed concentration of 58 µmol/ g of dry soil and the unrinsed CS had a sorbed concentration of 53 µmol/ g of dry soil. The final sorbed concentrations from columns of BS_0.2_50_1:1_COM and CS_0.2_50_1:1_COM are not included because there was an unexpected and large increase in aqueous ammonia concentrations after the 12th rinse treatment. This increase in ammonia concentrations is attributed to the falling head permeability measurement taken during the application of the last rinse treatment. Permeability measurements were taken using the effluent reservoirs which may have been contaminated from application of stimulation and cementation treatments. Therefore, it is also expected the sorbed ammonia would reflect higher and inaccurate concentrations.

The potassium chloride rinse proved to decrease the aqueous ammonia concentrations by 4 to 5 orders of magnitude in BS and CS columns. While there is no maximum allowable concentration of ammonia in drinking water, the US Environmental Protection Agency recommends a maximum of 1 mM and 0.1 mM total ammonia for acute and chronic exposure for aquatic life(U.S. Environmental Protection Agency 2013). For field scale trials if the priority was to reduce the ammonia by at least 90% then a total of 4 treatments would be necessary but if the priority was to reach maximum aqueous and sorbed concentration of 0.1 mM then about 12 treatment cycles would be necessary.

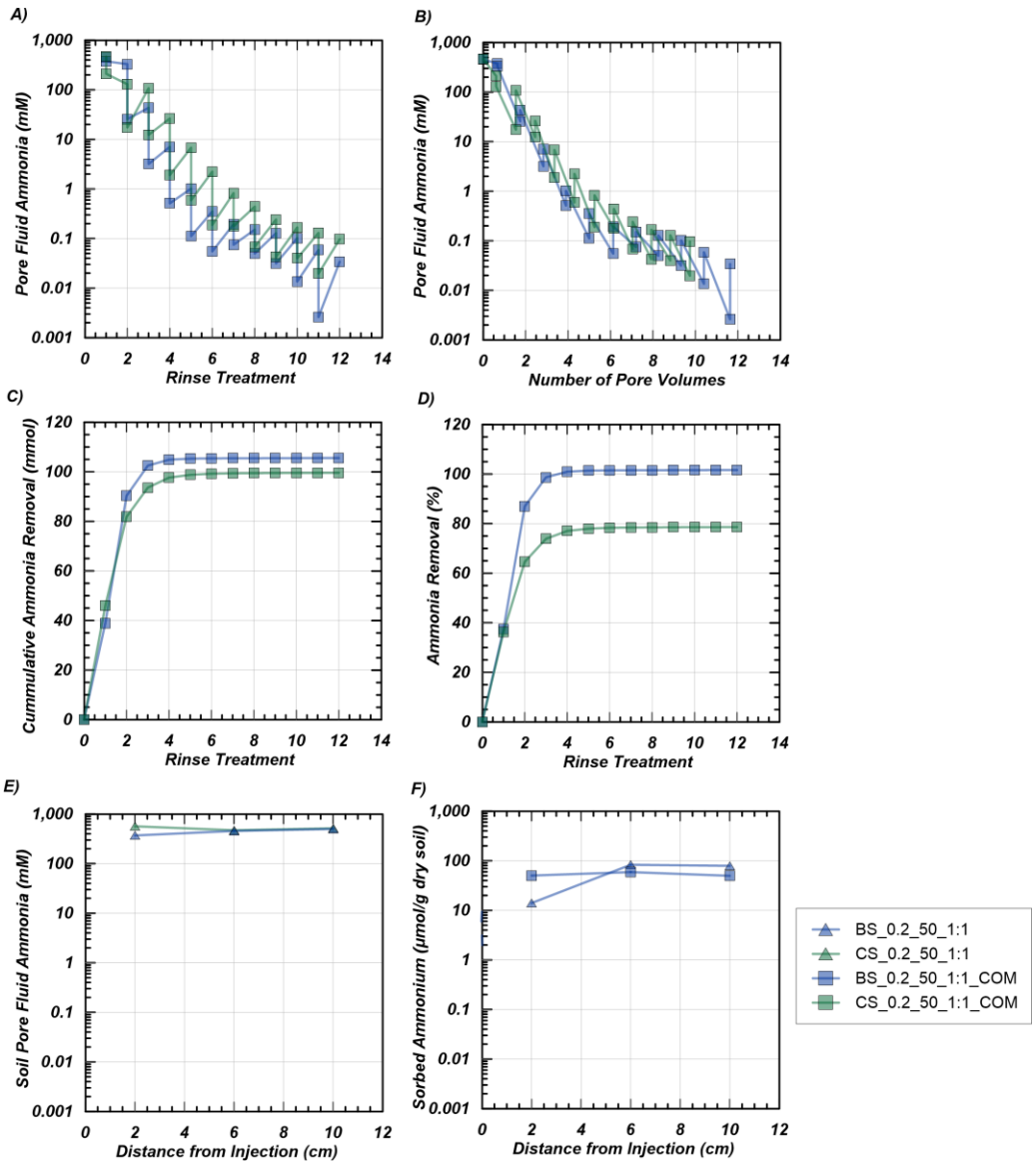

Figure 7: Changes in aqueous ammonia concentrations from the pore fluid of BS_0.2_50_1:1_COM and CS_0.2_50_1:1_COM versus (A) rinse treatment and (B) number of pore volumes. Ammonia removal versus rinse treatment in (C) cumulative ammonia concentration and (D) percent ammonia removal with respect to sorption concentration from unrinsed columns. Ammonia concentrations in unrinsed columns along the column length from the (E) soil pore fluid and (F) sorbed ammonia.

4.6 Shear Wave Velocity

Figure 8 presents shear wave velocity measurements during cementation treatments. Figure 8A shows the absolute measured V_s and Figure 8B presents the data as increase in shear wave velocity from the start of cementation. Blessington Sand had initial V_s between 80 m/s and 140 m/s with final V_s between 366 m/s and 472 m/s. Concrete Sand columns had an initial V_s near 200 m/s and final V_s values of 580 m/s and 610 m/s for columns CS_0.2_50_1:1_COM and CS_0.2_50_1:1, respectively. Accounting for the initial offsets in V_s from column packing, Blessington Sand columns had an increase in V_s between 294 m/s and 360 m/s while the Concrete Sand columns had an increase in V_s of 390 m/s for column CS_0.2_50_1:1 and 422 m/s for column CS_0.2_50_1:1_COM. In terms of increase in V_s, Concrete Sand achieved faster increase than the Blessington Sand due to the larger increases from the first 4 treatments. Considering that the biostimulation formulation was developed for Concrete Sand, it is not surprising that the response has an immediate effect. It is plausible that either additional stimulation treatments were needed to fully stimulate the Blessington Sand or the microbial population in the Blessington Sand is different from Concrete Sand and requires additional treatments to adjust to the new cementation solutions.

In both Figure 8A and 8B, the increase in V_s is linear between the 4th and final cementations. From the start of cementation to the 4th treatment, V_s in some columns such as BS_0.2_350_1.4:1 and BS_0.2_50_1:1_COM have a delay in the increase of V_s until they reach more uniform increase in V_s after the 4th treatment.

For the same chemical concentrations in the Blessington Sand and Concrete Sand, column BS_0.2_50_1:1 and CS_0.2_50_1:1 reach comparable increases in V_s of 360 m/s and 390 m/s, respectively. Column BS_0.2_50_1:1 had a uniform increase in V_s following the 2nd cementation while column CS_0.2_50_1:1 had the greatest increase in V_s during the first 2 cementations. This shows that for the

same chemical concentrations, both Blessington Sand and Concrete Sand can reach comparable levels of increase stiffness despite difference in pore space; however, Concrete Sand has a more significant increase in the first few treatments while Blessington Sand had a steady increase in stiffness over the course of cementation.

An increase in urea concentrations during stimulation did not result in a higher increase in V_s between column BS_0.2_50_1:1 and BS_0.2_350_1.4:1. Both columns achieved an increase in V_s of 351 m/s. This is comparable to the trends seen in pH where both columns were able to fully degrade urea by the 2nd stimulation treatment and remained in steady state for the remainder of the additional treatments.

By testing the lower limit of yeast extract concentration, column BS_0.02_350_1.4:1 was able to reach an increase in V_s of 346 which is comparable to the increase in Column BS_0.2_50_1:1 of 360 m/s while column BS_0.02_50_1:1 only reached an increase in V_s of 283 m/s. Consistent to the behavior seen in pH, column BS_0.02_50_1:1 was not able to establish bulk ureolytic activity until the 5th treatment. Despite not degrading the available urea in the first 5 treatments, the increase in V_s reflects some calcite precipitation occurring; however, it is not precipitation of the full 250 mM of calcium available. Despite the lower yeast extract concentrations in column BS_0.02_350_1.4:1, the increase is V_s was comparable to column BS_0.2_50_1:1 showing that the concentrations and number of treatments applied can serve as the lower bound for minimizing chemical concentrations to achieve comparable improvements.

Column BS_0.2_50_1:1 and BS_0.2_50_1:1_COM for Blessington Sand and column CS_0.2_50_1:1_COM reflect the difference between laboratory and industrial grade chemicals. The laboratory grade chemicals were expected to induce higher degrees of cementation than the industrial grade chemicals because the industrial grade chemicals are often less pure than the laboratory grade chemicals. Results followed expectations where the laboratory scale chemicals used in the Blessington

Sand reached V_s for column BS_0.2_50_1:1 of 359 m/s and 294 m/s in the commercial grade column BS_0.2_50_1:1_COM. For Concrete Sand, the commercial and laboratory grade columns were comparable as column CS_0.2_50_1:1_COM reflected a V_s increase of 423 m/s and column CS_0.2_50_1:1 reflected an increase 390 m/s. While the commercial grade column in Concrete Sands had a larger increase in V_s, the laboratory grade column had large increases in V_s over the first 4 treatments. Commercial grade columns yielded comparable increase in V_s in the Concrete Sands columns; however, the increase seen in the Blessington Sand was sufficient to increase soil stiffness. Additional cementation treatments for the commercial grade chemicals in Blessington Sand may be recommend to provide sufficient residence time to allow for further calcite precipitation.

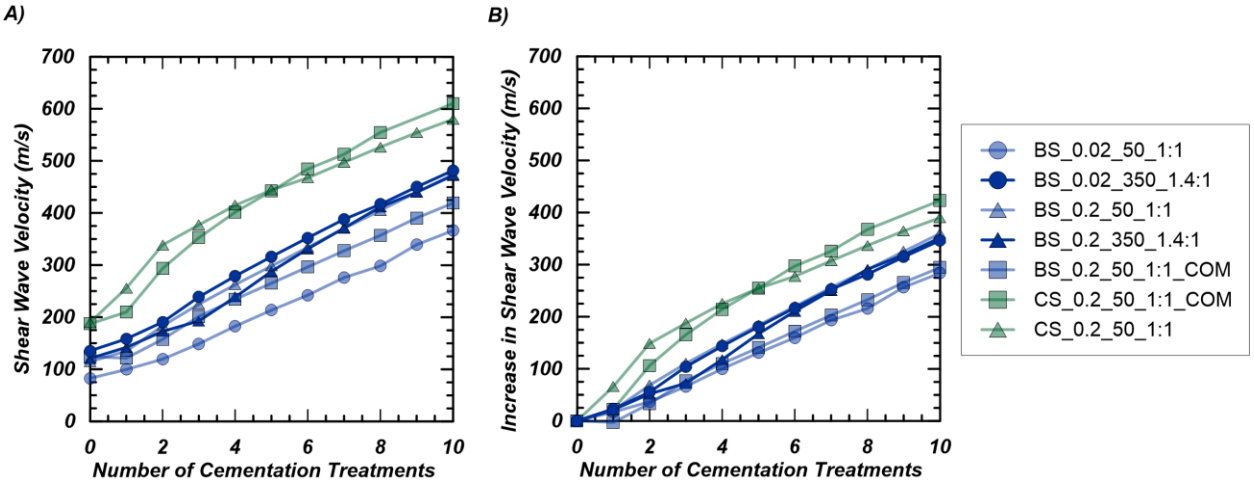

Figure 8: Measured (A) shear wave velocity and (B) increase in shear wave velocity during cementation treatments.

4.7 Calcite Content Distribution Along Column Length

Calcite contents along each column are shown in Figure 9. For both Blessington Sand and Concrete Sand columns, the increase in calcite contents ranged from 3.0 to 6.5% by mass. These values were determined by subtracting the measured calcite content from the untreated baseline values of Blessington Sand (28.9%) and Concrete Sand (0.1%). The calcite content distribution along the column length was more uniform in the Concrete Sand compared to the Blessington Sands. The Blessington Sand columns had higher calcite contents at the injection port which decreased further along the column. These trends are thought to be a reflection the larger porosity of the Concrete Sand compared to the Blessington Sand. It is also plausible that some transport of fines from the front to the latter part of the column may have occurred and contributed to the lower uniformity. While previous experiments have investigated treatment uniformity as a function of well spacing in Concrete Sands (San Pablo et al. 2020), further investigation is needed to understand optimal well spacing for carbonate sands as MICP applications are scaled for field trials to achieve uniform treatment in the target zone.

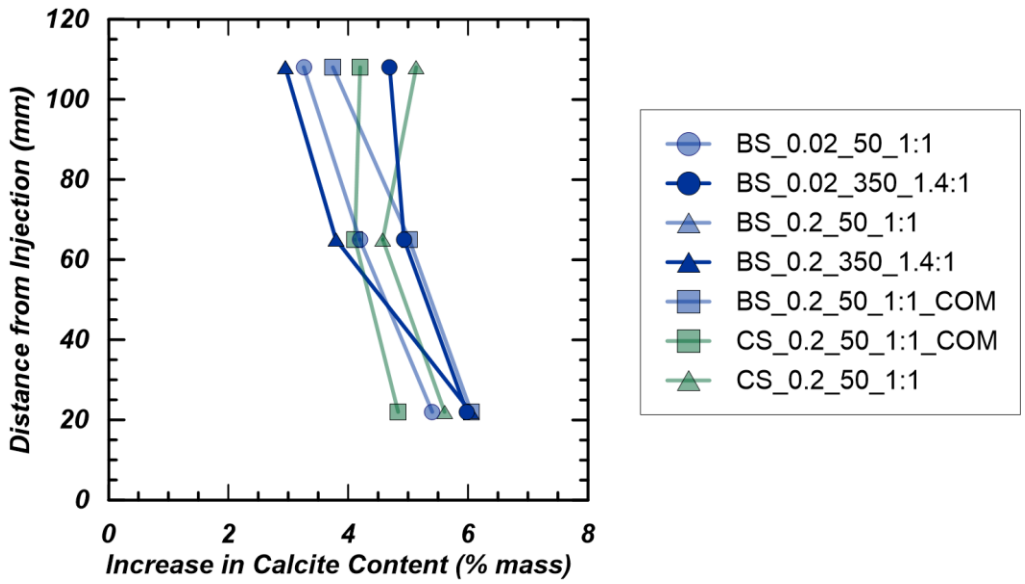

Figure 9: Measured increase in calcite content as a function of distance from treatment solution influent port.

4.8 Calcite Content Versus Change in V_s During Cementation

Comparison between shear wave velocity, normalized increase in shear wave velocity, increase in shear wave velocity per treatment and calcite contents are presented in Figure 10. For reference, Figure 10A and 10B include results from (Gomez et al. 2018a) where two 1.7 m tanks were used to treat Concrete Sand with bio-stimulation and bio-augmentation techniques. The increase in calcite content as a function various shear wave velocity benchmarks is significant in confirming increase in soil stiffness as a results of calcite precipitation via MICP. The shear wave velocity gives insight into increase in particle-to-particle contacts and the calcite content gives insight into calcite precipitation between particles. The combination of data sets allows the increase in soil stiffness to be attributed to the precipitation of calcite via MICP.

In Figure 10A, final shear wave velocity was plotted against increase in calcite content at column mid-height. In Gomez et al. (2018a) the uncemented V_s was near 115 m/s, the moderately cemented locations reached calcite contents of 3.0% and V_s near 500 m/s and the highly cemented locations reached calcite content of 5.25% and V_s near 900 m/s. Results from the current experiment ranged in V_s from 375m/s to 610 m/s and ranged in increase in calcite content from 3.8% to 5.5%

In Figure 10B, the change in shear wave velocity normalized to the uncemented shear wave velocity is plotted against the increase in calcite content at column mid-height. The trend line reflecting 100% percent change in normalized V_s per 1% increase in calcite content was developed in Gomez et al. (2018a) from results showing V_s improvements near 500% to increase in calcite content near 5.25%. The results from the current columns reflected an average 215% increase in V_s for a 4.3% increase in calcite content in the Concrete Sand columns and an average 288% increase in V_s for a 4.7% increase in calcite content in Blessington Sand columns. However, the differences observed using this normalization approach are primarily assignable to differences in the initial shear wave velocity or distribution of calcite precipitation along the column length.

In Figure 10C, the change in in shear wave velocity per treatment from cementation 4 to 10 when the columns reach a steady increase in V_s is plotted against the increase in calcite content at column mid-height. The increase in V_s over the final 5 cementation treatments ranged from 33 to 46 m/s for an increase in calcite content from 3.8% to 5.4%. Columns 1, 5, and 7 received lower concentration of urea stimulation and 1:1 urea: calcium during cementation, were on the lower bound of increase per cementation treatment with an increase of 36, 36 and 33 m/s respectively. Column BS_0.2_350_1.4:1 showed the highest increase in V_s of 46 m/s per treatment as expected given the highest urea to calcium concentrations.

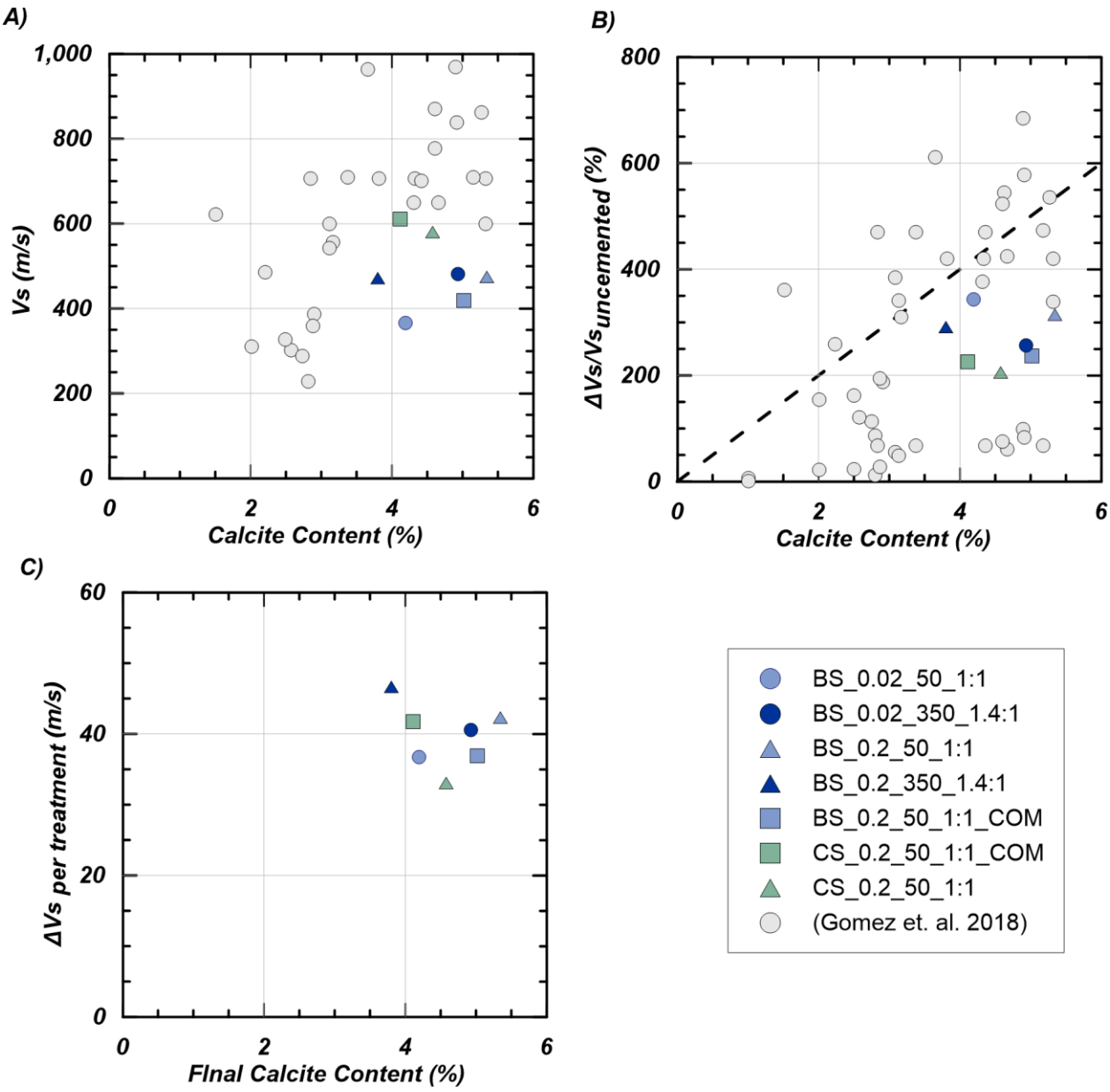

Figure 10: Increase in calcite content as a function of (A) shear wave velocity, (B) normalized increase in shear wave velocity, and (C) increase in shear wave velocity per treatment.

4.9 Strength

The results for unconfined compressive strengths for columns BS_0.02_50_1:1, BS_0.02_350_1.4:1 and BS_0.2_350_1.4:1 are presented in Figure 11. The maximum compressive strengths increased with increasing yeast extract and urea concentrations. Columns BS_0.02_50_1:1, BS_0.02_350_1.4:1 and BS_0.2_350_1.4:1 reach maximum compressive strengths of 0.40, 0.58 and 0.68 MPa, respectively. The maximum compressive strengths are on the lower end of strengths reported in similar experiments (Gomez and DeJong 2017); however, it should be noted that this may be attributed to the sample disturbance that occurred during hydraulic jacking during the sample extrusion process. While the compressive strengths followed the expected trend of increased strength with increased chemical concentrations, the increase in calcite content for the respective columns did not follow the same trend as column BS_0.2_350_1.4:1 had an increase in calcite content of 3.8%.

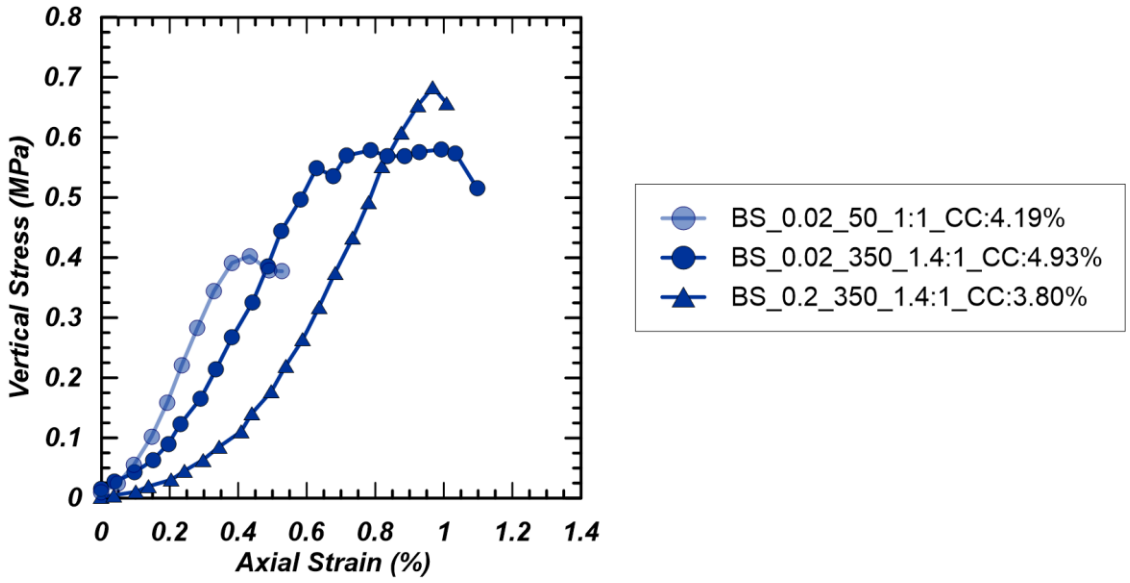

Figure 11: Unconfined compressive strengths for BS_0.02_50_1:1, BS_0.02_350_1.4:1, and BS_0.2_350_1.4:1.

4.10 Permeability

Results from falling head test resulted in permeability of 8.1E-05 cm/sec to 1.5E-04 cm/sec for Blessington Sand columns and 2.1E-04 cm/sec to 6.4E-04 cm/sec for Concrete Sand Columns. This range of permeability values are typically categorized as poor drainage in fine sands and silts (Holtz and Kovacs 1981). Initial permeability were obtained during initial saturation however, the values do not accurately reflect initial permeability since some fines washed out from the columns during the first stimulation treatments.

4.11 LOI & TGA

Results for LOI are presented in Table 4 for untreated and treated soil samples. These tests were run in a one stage process where the loss in mass is calculated as the mass of CO_2 loss from heating samples up to 950 °C for 2 hours. The total mass loss was 13.26% for untreated BS and 2.93% for untreated CS. If it is assumed that all loss was due to calcium carbonate then calcite content for untreated BS and CS were 30.14% and 6.67% respectively. Calcium carbonate was calculated by assuming 100.9 g of CaCO3 released 44.01 g of CO_2 and all loss in CO_2 was a results of calcium carbonate decomposition. Therefore, the treated BS columns has calcite content ranging from 35.23% to 36.42%, which is a 5.09% to 6.28% increase due to MICP treatment. The CS columns reached calcite content of 7.66% to 8.18%, which is 0.99% to 1.51% increase in calcite content due to MICP treatments. The range of 4.50% to 6.28% increase in calcite content for treated BS samples is comparable to the increase found using the acid wash method in Figure 9. The acid wash method yielded calcite contents ranging from 3.5% to 5.5%, which is slightly lower than seen in LOI; however, with the single stage LOI up to 950 °C there is a possibility the mass loss is due to decomposition of other compounds. Increase in calcite content for treated samples were also expected to be comparable to the acid wash calcite contents of 3.5% to 5.5%. Therefore, the range of 0.99% to 1.51% increase in calcite content for treated CS samples is lower than expected values. The CS samples were run a second time and results fluctuated +/- 4% in mass lost. Since LOI was conducted in a

single stage process, the TGA provides more insight into the mass lost in temperature ranges specific to the breakdown of calcite.

TGA was conducted to provide a more refined analysis for mass loss at specific temperature ranges. Results for TGA are presented in Figure 12 and 13. Figure 12 presents the raw data for mass lost for untreated BS in Figure 12A, untreated CS in Figure 12B, treated BS samples in Figure 12C, and treated CS samples in Figure 12D. Figure 13 presents the percent mass lost to normalize for sample size. Figure 13A and 13B present the normalized TGA for all BS and CS samples, respectively. Figures 13C and 13D present the normalized DTG (differential mass lost) for all BS and CS samples, respectively. For reference, the data set also includes TGA and DTG curves for pure calcite from Li et al. (2017) and Villagrán-Zaccardi et. al. (2017).

The TGA data show BS loses most of the mass above 700°C in both the untreated and treated columns. This is consistent with the expectations that the soil is primarily comprised of silica and carbonate. The CS samples have significant loss in mass from 450°C to 700°C, and very little mass loss due to the decomposition of calcium carbonate. The TGA results from Li et. al (2017) align more with the trends seen in the BS and CS results. The significant loss in mass for the pure calcite from Li et. al (2017) begins around 650°C where the significant loss in mass occurs closer to 750°C for pure calcite from Villagrán-Zaccardi et. al. (2017). The BS and CS untreated and treated samples reflect the most significant mass lost starting at 650°C. Both Li et al. (2017) and Villagrán-Zaccardi et. al. (2017) specified the calcium carbonate used was reagent grade, therefore differences in decomposition may be due to crystal structures.

Literature also suggests methods to estimate the calcite contents from TGA results. Table 5 presents the results for Calcite contents of pure calcite, untreated and treated soil samples. The first method was proposed by Villagrán-Zaccardi et. al. (2017) where the mass loss from the distance at the

inflection point on the TGA curve is calculated between the tangent drawn from the curve before and after the significant change in slope. Then the mass lost is converted assuming the release of 44.01 g of CO_2 is released for every 100.09 g of Ca CO_2. Villagrán-Zaccardi et. al. (2017)'s method assumes there is partial decarbonation between 400°C to 600°C forming CaO and calcite. Therefore, poorly crystalized carbonates decomposed at lower temperatures (400°C to 600°C) and well-crystalized calcite decomposes at higher temperatures (600°C to 800°C). The second method proposed by Li et. al. (2017) only attributes the mass CO_2 lost from 600°C to 850°C degrees to calcite decomposition.

The method proposed by Villagrán-Zaccardi et. al. (2017) yields calcite contents of 32.6% for untreated BS, 34.5% to 36.9% for treated BS, 4.0% for untreated CS and 17.7% to 35.4% for treated CS. The method proposed by Li et. al. (2017) yields calcite contents of 22.0% for untreated BS, 17.8% to 29.4% for treated BS, 5.1% for untreated CS and 10.5% to 22.3% for treated CS. The calcite contents determined using Villagrán-Zaccardi et. al. (2017)'s method more accurately aligns with the calcite contents determined from the acid washing method used in Figure 9 and LOI presented in Table 4. However, there are large differences in the calcite content found for treated and untreated CS in comparison to the acid washing method. This may be attributed to the small and non-representative sample size used to run TGA.

Table 4: Loss on ignition results for untreated and treated samples.

Column	Loss in Mass (%)	Calculated Calcite Content (%)	Calculated Increases in Calcite Content (%)
Blessington Sand Untreated	13.26	30.14	-
Concrete Sand Untreated	2.93	6.67	-
BS_0.02_50_1:1	16.02	36.42	6.28
BS_0.02_350_1.4:1	15.66	35.59	5.45
BS_0.2_50_1:1	15.86	36.04	5.90
BS_0.2_350_1.4:1	15.81	35.93	5.79
BS_0.2_50_1:1_COM	15.50	35.23	5.09
CS_0.2_50_1:1_COM	3.60	8.18	1.51
CS_0.2_50_1:1	3.37	7.66	0.99

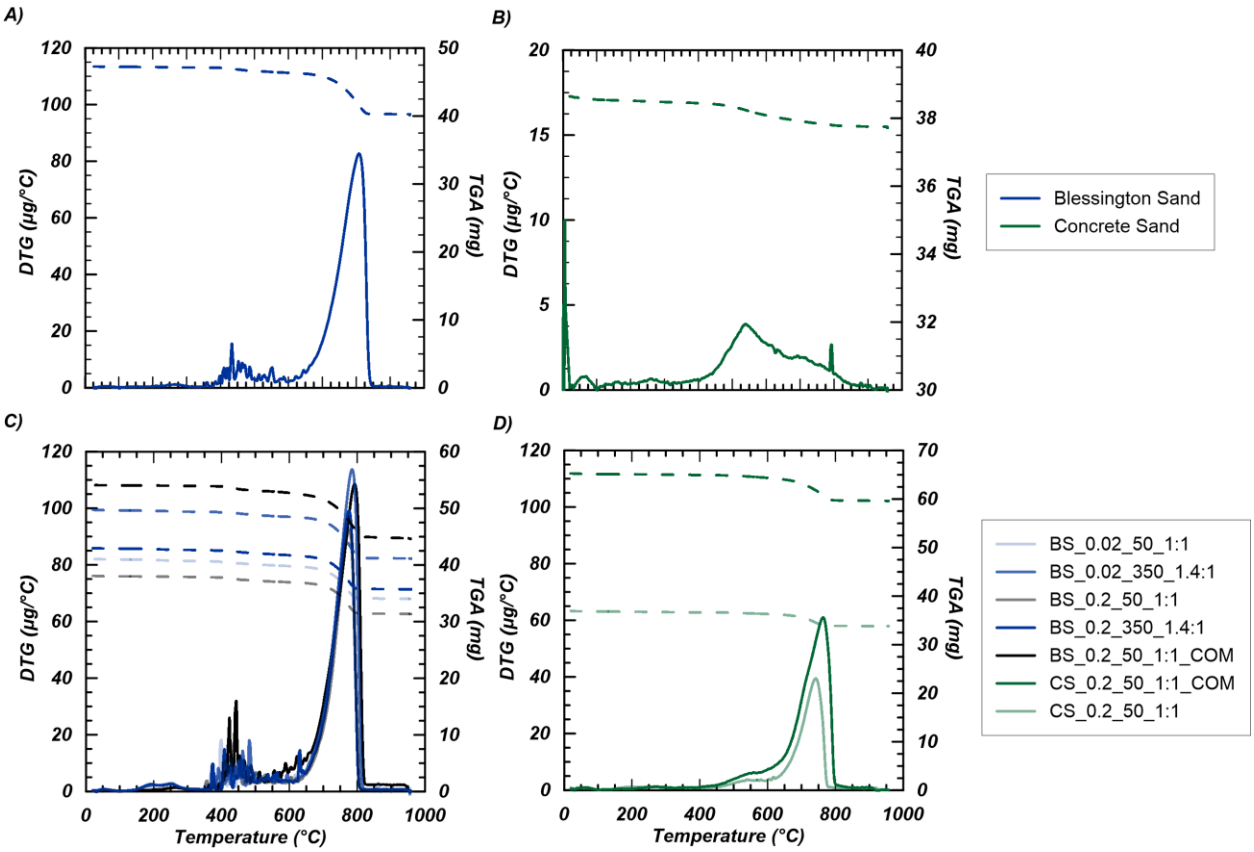

Figure 12: Thermogravimetric (TGA) measurements for (A) untreated Blessington Sand, (B) untreated Concrete Sand, (C) treated Blessington Sand columns, and (D) treated Concrete Sand Columns. Solid lines are DTG and dashed lines are TGA. Tests performed by Prof. Susan Burns research group (Georgia Institute of Technology).

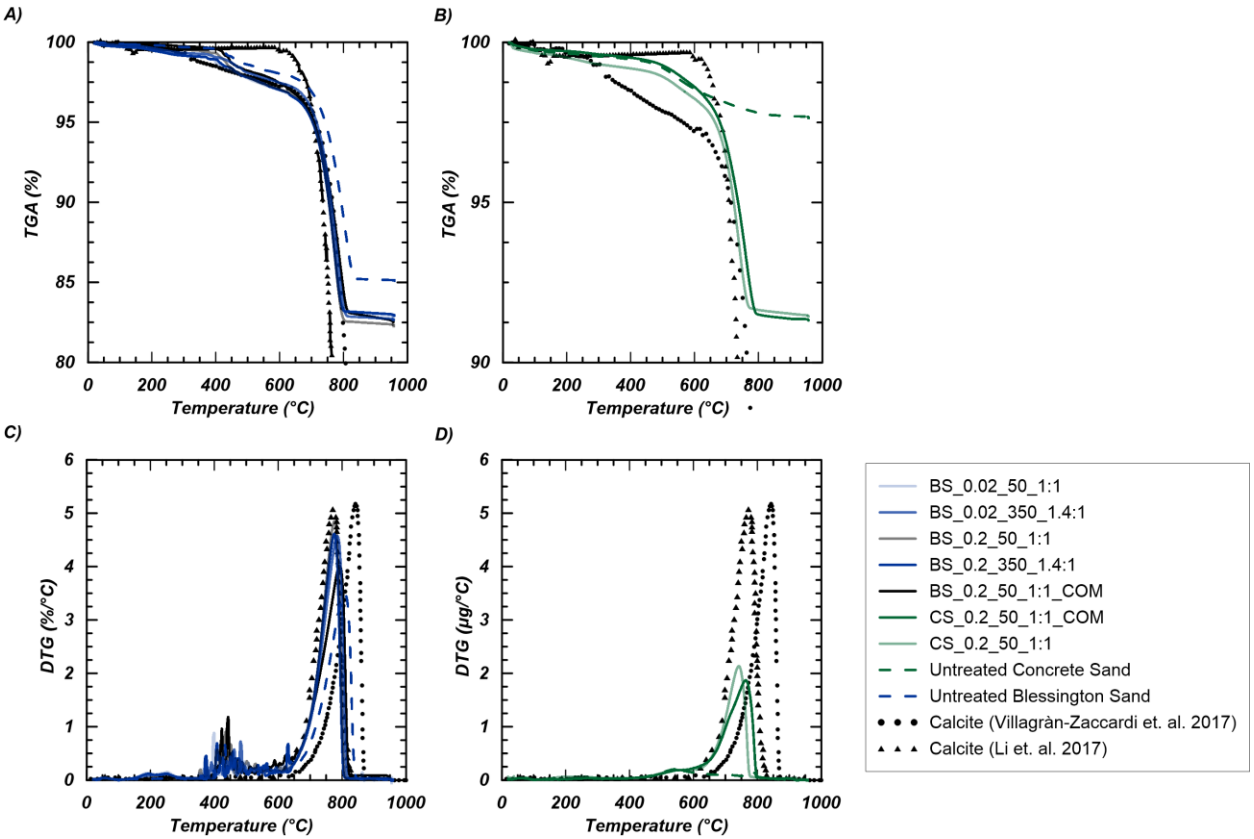

Figure 13: Normalized thermogravimetric measurements for pure calcite, untreated and treated soil samples. TGA and DTG for (A & C) treated and un untreated Blessington Sand and (B & D) treated and untreated Concrete Sand, respectively. Tests performed by Prof. Susan Burns research group (Georgia Institute of Technology).

Table 5: Calcite content TGA for untreated and treated soil samples.

Column	Calcite Content (%)[1]	Calcite Content (%)[2]
Blessington Sand Untreated	32.6	22.0
Concrete Sand Untreated	4.0	5.1
BS_0.02_50_1:1	36.0	29.1
BS_0.02_350_1.4:1	36.1	27.2
BS_0.2_50_1:1	36.9	29.4
BS_0.2_350_1.4:1	34.5	21.8
BS_0.2_50_1:1_COM	37.3	17.8
CS_0.2_50_1:1_COM	17.7	10.5
CS_0.2_50_1:1	35.4	22.3
Pure Calcite Villagrán-Zaccardi et. al. (2017)	93.8	80.8
Pure Calcite Li et. al. (2017)	100.0	84.1

[1]Calculated using tangential method from Villagrán-Zaccardi et. al. (2017).
[2]Calculated using Li et. al. (2017).

4.12 SEM

Figure 14 present SEM images from all columns and untreated samples. SEM images were taken with magnification ranging from 30x to 1,000x. While these images do not give insight into the crystal structure of the calcite precipitates, the comparison of soil surfaces between the untreated samples to the treated samples suggests the presents of calcite crystals. Both the untreated BS and CS reflect angular particles with some smooth surfaces. The treated samples have rough surfaces due to the presence of small crystals, which are assumed to be calcite precipitates.

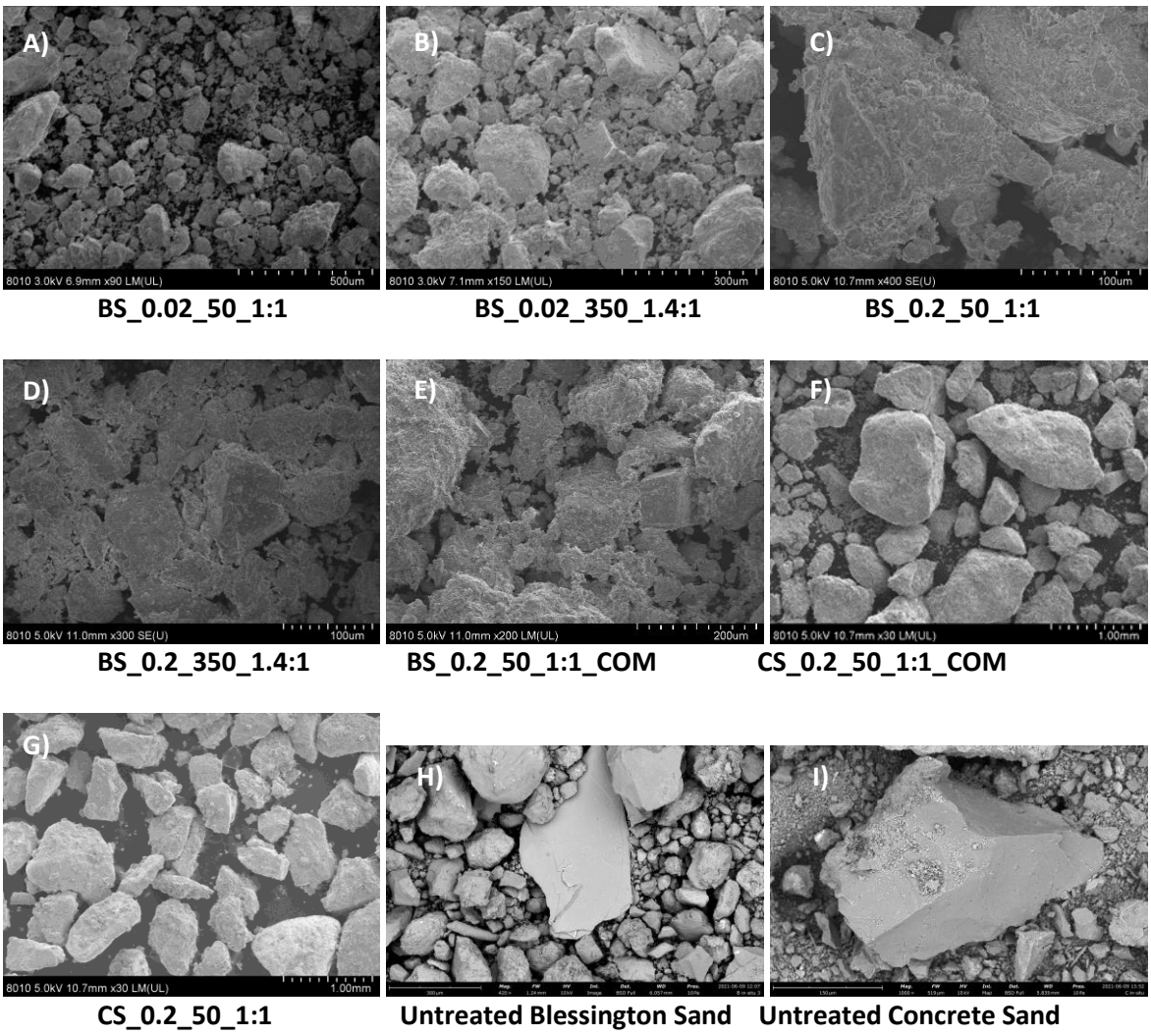

Figure 14: SEM of crushed soil samples at (A) 90x, (B) 150x, (C) 400x, (D) 300x, (E) 200x, (F & G) 30x, (H) 420x, and (I) 1,000x magnification. Tests performed by Prof. Susan Burns research group (Georgia Institute of Technology).

4.13 XRD

Figure 15 and 16 present XRD scans from all columns and untreated samples. The soil samples were only scanned for quartz and calcite although literature suggests there may also be kaolinite, undefined forms of iron, and zirconium in BS (Igoe and Gavin 2019). The percentage of quartz and calcite was determined for each XRD scan. The percentage was summed to 100% and does not account for any unidentified minerals from the red peaks in the raw scans. These scans suggest calcite content of 25.8% in the untreated BS and 23.5% to 77.7% calcite in the treated samples. The CS columns reflect 0% calcite in the untreated sample and 4.3% to 9.7% in the treated samples. These data show an increase in calcite for all treated samples except column BS_0.02_50_1:1. However, the calculated percent calcite from the XRD scans do not fully encompass other minerals that maybe present in the sample, and thus cannot reflect absolute calcite contents. Additional studies on the geology and mineralogy of BS are necessary to obtain more information from the XRD scans.

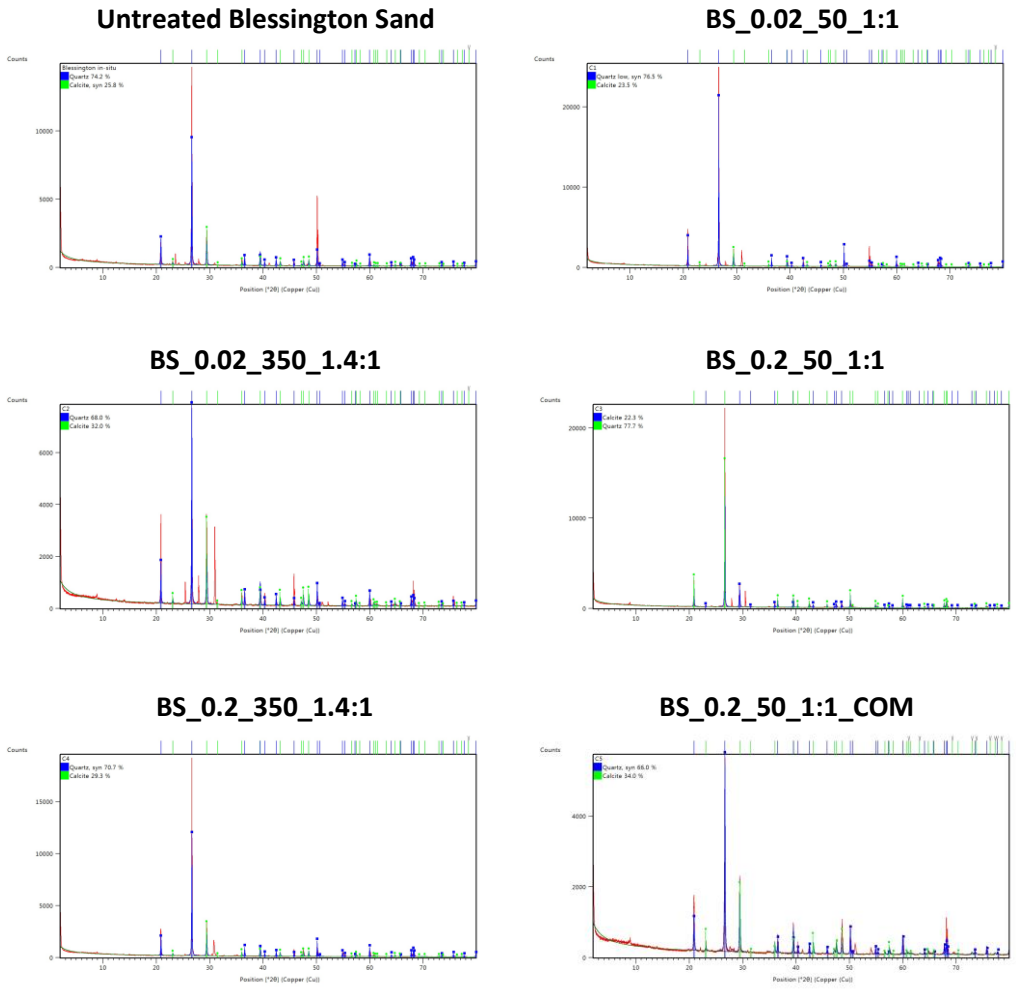

Figure 15: XRD patterns for untreated soils and MICP treated soils. Red line: intensity from raw data; Bue line: Quartz; Green line: Calcite. (A) Untreated Blessington Sand, (B) BS_0.02_50_1:1, (C) BS_0.02_350_1.4:1, (D) BS_0.2_50_1:1, (E) BS_0.2_350_1.4:1, and (F) BS_0.2_50_1:1_COM. Tests performed by Prof. Susan Burns research group (Georgia Institute of Technology).

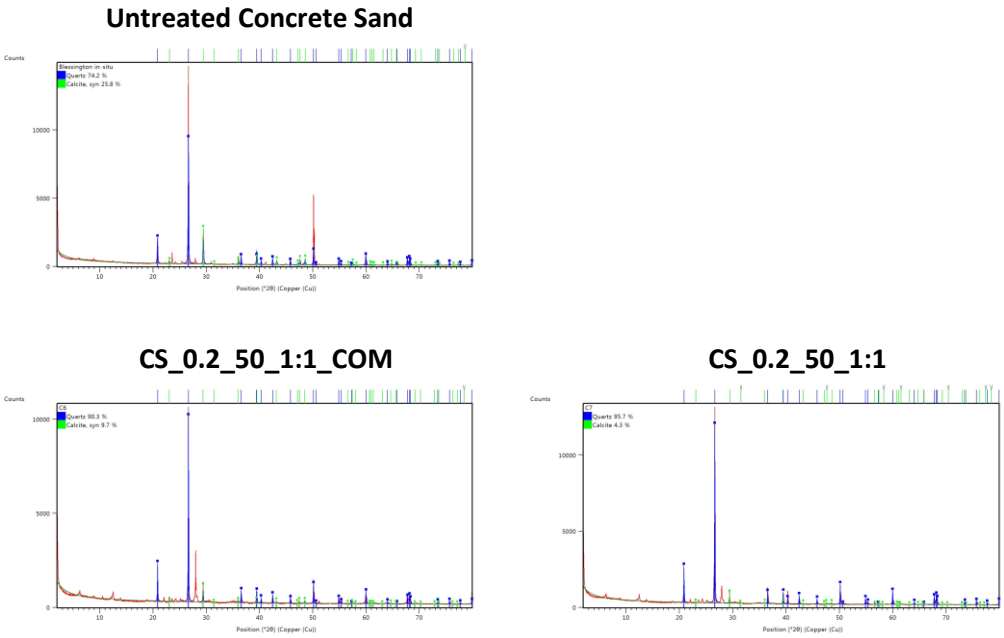

Figure 16: XRD patterns for untreated soils and MICP treated soils. Red line: intensity from raw data; Bue line: Quartz; Green line: Calcite. (A) Untreated Concrete Sand, (B) CS_0.2_50_1:1_COM, and (C) CS_0.2_50_1:1. Tests performed by Prof. Susan Burns research group (Georgia Institute of Technology).

4.14 EDS

Figure 17 and 18 present EDS for BS and CS samples, respectively. From Figure 17 it can be deduced that the treated BS samples contained carbon, calcium, oxygen, iron, aluminum and silica. The untreated BS sample contained the same elements with additional traces of potassium and sodium. From Figure 18 the treated CS samples contained carbon, calcium, oxygen, iron, aluminum, silica, magnesium and chorine. The untreated concrete sample contained traces of oxygen, iron, aluminum, silica, potassium, calcium and titanium. The images used for the EDS were taken between 599x and 1249x magnification. The calcite crystal structures do not have significant difference in shape between the commercial and laboratory grade chemicals or between the soil types.

Untreated Blessington Sand

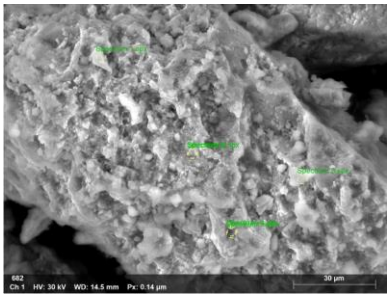

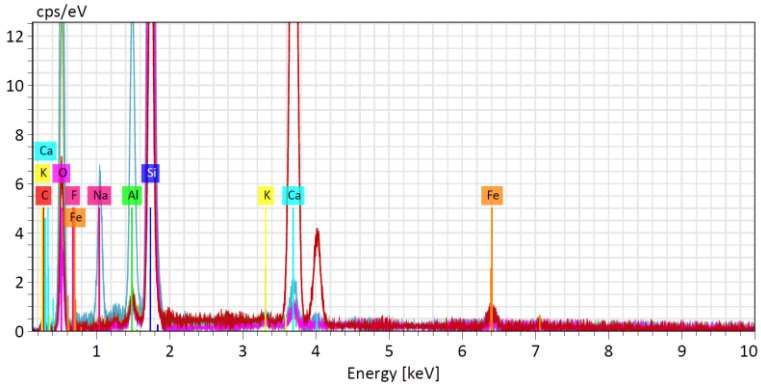

BS_0.2_50_1:1

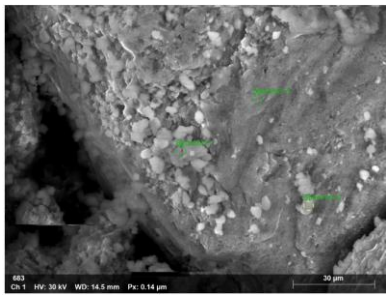

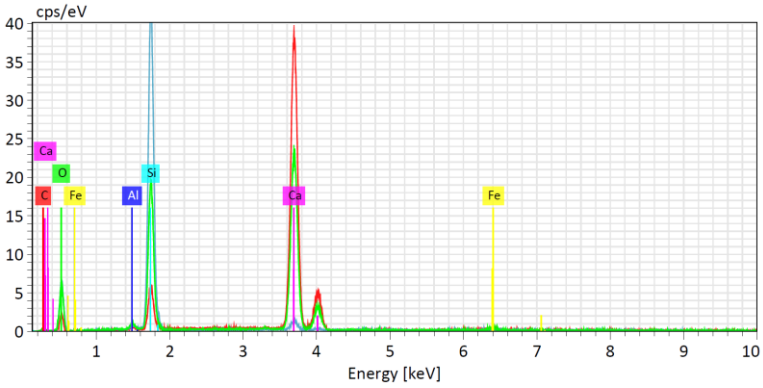

BS_0.2_50_1:1_COM

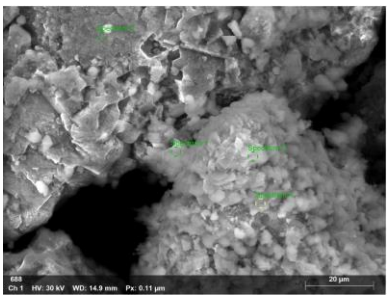

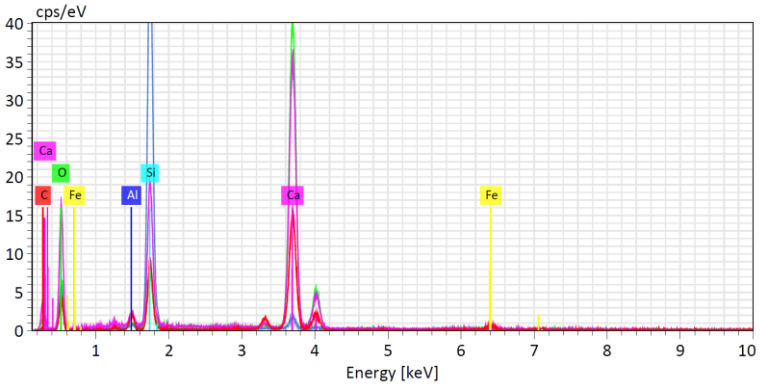

Figure 17: EDS of Untreated Blessington Sands, BS_0.2_50_1:1 and BS_0.2_50_1:1_COM taken with 999x, 999x, and 1249x magnification, respectively.

Untreated Concrete Sand

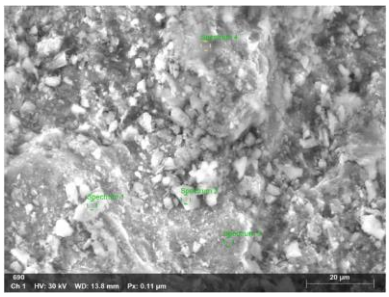

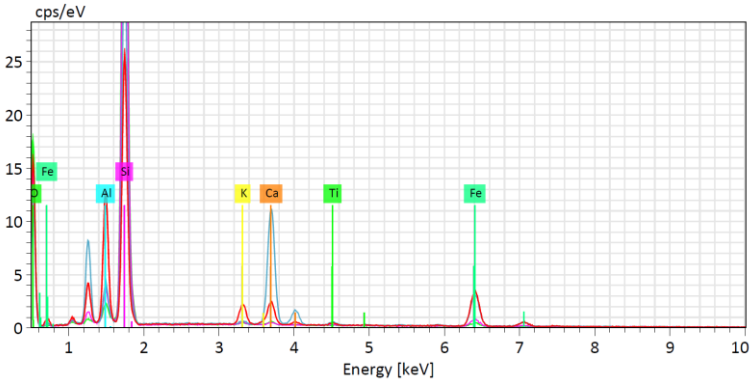

CS_0.2_50_1:1

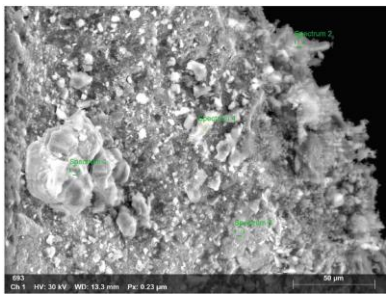

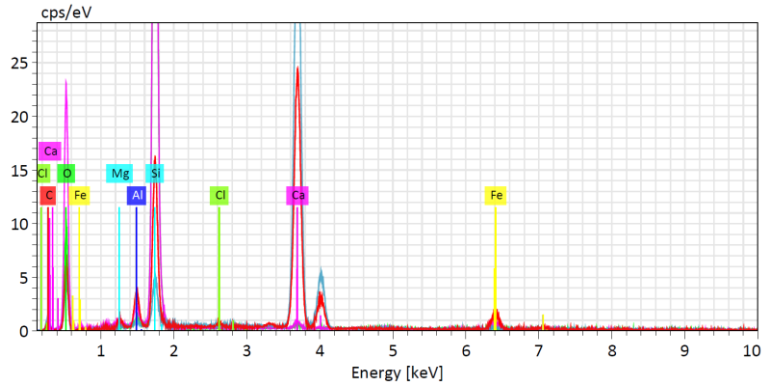

CS_0.2_50_1:1_COM

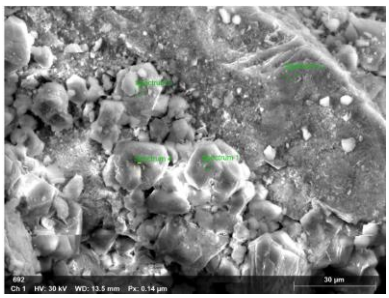

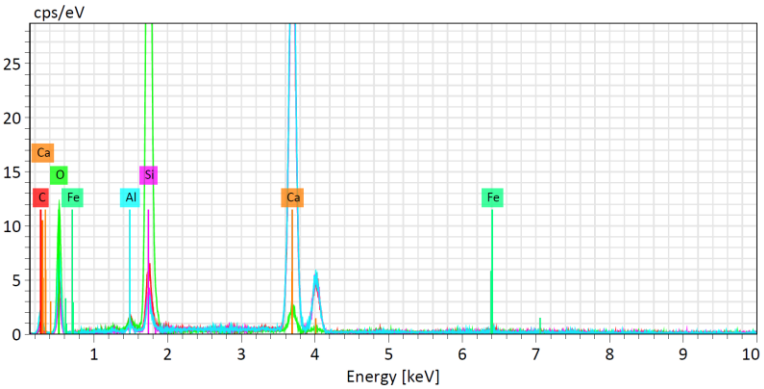

Figure 18: EDS of Untreated Concrete Sands, CS_0.2_50_1:1 and CS_0.2_50_1:1_COM taken with 1249x, 599x, and 999x magnification, respectively.

5. CONCLUSIONS

A study was completed using seven centimeter-scale columns containing Blessington Sands and Concrete Sands to (1) improve our understanding of the robustness of bio-stimulation in carbonate particles, (2) evaluate the effectiveness of commercial grade chemicals and (3) understand the effectiveness of byproduct removal. Based on the results of this experiment, the following conclusions can be made:

1. Results of pH analyses show that bio-stimulation in BS is comparable to results seen in previous CS experiments whereby stimulation treatments signify the presence of high ureolytic activity by producing a pH of 9.3 and full urea degradation at a pH upwards of 8.0 for cementation treatments. Values of pH highlighted the lag in establishing ureolytic activity in the low YE and low Urea column, BS_0.02_50_1:1.

2. Urea degradation showed that the robustness of bio-stimulation in BS and CS was comparable between the commercial and laboratory grade chemicals. Urea degradation rates also highlighted the need for additional stimulation treatments for the low YE columns (BS_0.02_50_1:1 and BS_0.02_350_1.4:1) to provide sufficient residence time to reach at least 90% urea degradation before transitioning to cementation treatments. The zeroth-order and first-order kinetics suggest the ureolysis rates for high YE columns with BS and CS were comparable and increased with additional treatments.

3. Potassium chloride rinsing for columns BS_0.2_50_1:1_COM and CS_0.2_350_1:1 suggest that 12PV of treatment over 12-days allows for aqueous ammonia levels to decrease to 0.03 mM and sorbed ammonia to decrease 0.01 µmol/g, resulting in a 99% decrease in the ammonia present at the end of cementation treatments. The ability to decrease ammonia concentrations suggests that concentrations of these byproducts are low enough that they should not be an environmental

concern for field-scale MICP applications, as they meet the EPA's criteria of less than 0.1 mM in drinking water.

4. Increases in shear wave velocities showed that low YE columns, BS_0.02_50_1:1 and BS_0.02_350_1.4:1, had some degree of calcite precipitation during the first cementation treatments despite an inability to fully degrade the available urea. Results also suggest that there were uniform increases in V_s from cementation treatments 6 to 10 for all columns, despite differences in soil type and chemical concentrations.

5. Calcite contents obtained using the acid washing method suggest an increase of between 3.5% to 5.5% in BS and 4.0% to 4.5% in CS. This increase was comparable to previous experiments conducted on CS. In comparison to increase in V_s, results showed the increase in V_s can be attributed to the increase in particle to particle contact through the formation of calcite precipitates. Calcite content measured as a function of distance from treatment injection in BS suggest that well spacing for field scale trials should be further investigated as the solution transport is not as effective as seen in CS.

6. Unconfined compressive strengths suggest that increases in YE, urea and calcium chloride concentrations result in an increase in compressive strengths for BS, as seen in previous experiments for CS.

7. LOI and TGA provided alternative methods to confirm high calcite contents in BS samples. Villagrán-Zaccardi et. al. (2017)'s method for determining calcite contents aligns closely with the acid washing method and the LOI results in treated BS samples with calcite contents from 34.5% to 36.9%. However, there were discrepancies in the treated CS where LOI reflected 7.66% to 8.18% calcite content and TGA reflected 10.5% to 22.3% calcite content.

8. SEM, XRD and EDS suggest the formation of calcite precipitates on the soil particle surfaces. There was no significant difference in the crystal structure between the laboratory and commercial grade chemicals. Further geology and mineralogy studies are required to reach a better understanding of the minerals present in BS.

6. REFERENCES

ASTM International. (2013). *Test Methods for Loss on Ignition (LOI) of Solid Combustion Residues*. ASTM International.

ASTM International. (2014). *Test Method for Rapid Determination of Carbonate Content of Soils*. ASTM International.

Burbank, M., Weaver, T., Green, T., Williams, B., and Crawford, R. (2011). "Precipitation of calcite by indigenous icroorganisms to strengthen liquefiable soils." *Geomicrobiology Journal*, 28(4), 301–312.

Burbank, M., Weaver, T., Lewis, R., Williams, T., Williams, B., and Crawford, R. (2013). "Geotechnical Tests of Sands Following Bioinduced Calcite Precipitation Catalyzed by Indigenous Bacteria." *JOURNAL OF GEOTECHNICAL AND GEOENVIRONMENTAL ENGINEERING*, 139(6), 928–936.

Casas, C. C., Schaschke, C. J., Akunna, J. C., and Ehsan Jorat, M. (2019). "Dissolution experiments on dolerite quarry fines at low liquid-to-solid ratio: a source of calcium for MICP." *Environmental Geotechnics*, 1–9.

Chaney, R., Demars, K., Brignoli, E., Gotti, M., and Stokoe, K. (1996). "Measurement of Shear Waves in Laboratory Specimens by Means of Piezoelectric Transducers." *Geotechnical Testing Journal*, 19(4), 384.

Cuthbert, M. O., McMillan, L. A., Handley-Sidhu, S., Riley, Michael. S., Tobler, D. J., and Phoenix, Vernon. R. (2013). "A Field and Modeling Study of Fractured Rock Permeability Reduction Using Microbially Induced Calcite Precipitation." *Environmental Science & Technology*, 47(23), 13637–13643.

Darby, K. M., Hernandez, G. L., DeJong, J. T., Gomez, M. G., and Wilson, D. W. (2019). "Centrifuge Model Testing of Liquefaction Mitigation via Microbially Induced Calcite Precipitation." *J. Geotech. Geoenviron. Eng.*, 144(10), 13.

DeJong, J. T., Fritzges, M. B., and Nusslein, K. (2006). “Microbial induced cementation to control sand response to undrained shear.”

Dyer, M., and Viganotti, M. (2017). “Oligotrophic and eutrophic MICP treatment for silica and carbonate sands.” *Bioinspired, Biomimetic and Nanobiomaterials*, 6(3), 168–183.

Fang, X., Yang, Y., Chen, Z., Liu, H., Xiao, Y., and Shen, C. (2020). “Influence of Fiber Content and Length on Engineering Properties of MICP-Treated Coral Sand.” *Geomicrobiology Journal*, 37(6), 582–594.

Feng, K., and Montoya, B. M. (2017). “Quantifying Level of Microbial-Induced Cementation for Cyclically Loaded Sand.” *J. Geotech. Geoenviron. Eng.*, 4.

Ferris, F. G., Pheonix, V., Fujita, Y., and Smith, R. W. (2004). “Kinetics of calcite precipitation induced by ureolytic bacteria at 10 to 20°C in artificial groundwater.” *Geochim. Cosmochim. Acta.*, 67(8), 1701–1722.

Fujita, Y., Taylor, J. L., Gresham, T. L. T., Delwiche, M. E., Colwell, F. S., McLing, T. L., Petzke, L. M., and Smith, R. W. (2008). “Stimulation Of Microbial Urea Hydrolysis In Groundwater To Enhance Calcite Precipitation.” *Environmental Science & Technology*, 42(8), 3025–3032.

Gomez, M. G., Anderson, C. M., DeJong, J. T., Nelson, D. C., and Lau, X. H. (2014). “Stimulating In Situ Soil Bacteria for Bio-Cementation of Sands.” *Geo-Congress 2014 Technical Papers*, American Society of Civil Engineers, Atlanta, Georgia, 1674–1682.

Gomez, M. G., and DeJong, J. T. (2017). “Engineering Properties of Bio-Cementation Improved Sandy Soils.” *Grouting 2017*, American Society of Civil Engineers, Honolulu, Hawaii, 23–33.

Gomez, M. G., DeJong, J. T., and Anderson, C. M. (2018a). “Effect of bio-cementation on geophysical and cone penetration measurements in sands.” *Canadian Geotechnical Journal*, 55(11), 1632–1646.

Gomez, M. G., DeJong, J. T., Anderson, C. M., Nelson, D. C., and Graddy, C. M. (2016). "Large-Scale Bio-Cementation Improvement of Sands." *Geotechnical and Structural Engineering Congress 2016*, American Society of Civil Engineers, Phoenix, Arizona, 941–949.

Gomez, M. G., Graddy, C. M. R., DeJong, J. T., and Nelson, D. C. (2019). "Biogeochemical Changes During Bio-cementation Mediated by Stimulated and Augmented Ureolytic Microorganisms." *Scientific Reports*, 9(1), 11517.

Gomez, M. G., Graddy, C. M. R., DeJong, J. T., Nelson, D. C., and Tsesarsky, M. (2018b). "Stimulation of Native Microorganisms for Biocementation in Samples Recovered from Field-Scale Treatment Depths." *Journal of Geotechnical and Geoenvironmental Engineering*, 144(1), 04017098.

Graddy, C. M. R., Gomez, M. G., DeJong, J. T., and Nelson, D. C. (2021). "Native Bacterial Community Convergence in Augmented and Stimulated Ureolytic MICP Biocementation." *Environmental Science & Technology*, acs.est.1c01520.

Graddy, C. M. R., Gomez, M. G., Kline, L. M., Morrill, S. R., DeJong, J. T., and Nelson, D. C. (2018). "Diversity of *Sporosarcina* -like Bacterial Strains Obtained from Meter-Scale Augmented and Stimulated Biocementation Experiments." *Environmental Science & Technology*, 52(7), 3997–4005.

Han, Z., Xiaohui, C., and Qiang, M. (2016). "An experimental study on dynamic response for MICP strengthening liquefiable sands." *Eartquake Engineering and Egineering Vibration*, 7.

Holtz, R. D., and Kovacs, W. D. (1981). *An introduction to geotechnical engineering*.

Igoe, D., and Gavin, K. (2019). "Characterization of the Blessington sand geotechnical test site." *AIMS Geosciences*, 5(2), 145–162.

Keeney, D. R., and Nelson, D. W. (1982). "Nitrogen-Inorganic Forms 1." *Methods of soil analysis. Part 2. Chemical and microbiological properties*, 643–698.

Knorst, M. T., Neubert, R., and Wohlrab, W. (1997). “Analytical methods for measuring urea in pharmaceutical formulations.” *Journal of Pharmaceutical and Biomedical Analysis*, 15(11), 1627–1632.

Krom, M. D. (1980). “Spectrophotometric determination of ammonia: a study of a modified Berthelot reaction using salicylate and dichloroisocyanurate.” *The Analyst*, 105(1249), 305.

Lee, J.-S., and Santamarina, J. C. (2005). “Bender Elements: Performance and Signal Interpretation.” *Journal of Geotechnical and Geoenvironmental Engineering*, 131(9), 1063–1070.

Lee, M., Gomez, M. G., Graddy, M. R., DeJong, J. T., and Nelson, D. C. (2019). “Investigating Ammonium By-product Removal for Ureolytic Bio-cementation Soil Improvement Using Meter-Scale Experiments.” *Scientific Reports*, 9(18313), 25.

Lei, X., Lin, S., Meng, Q., Liao, X., and Xu, J. (2020). “Influence of different fiber types on properties of biocemented calcareous sand.” *Arabian Journal of Geosciences*, 13(8), 317.

Li, Y., Guo, Z., Wang, L., Li, Y., and Liu, Z. (2020). “Shear resistance of MICP cementing material at the interface between calcareous sand and steel.” *Materials Letters*, 274, 128009.

Li, Y., Guo, Z., Wang, L., Ye, Z., Shen, C., and Zhou, W. (2021). “Interface Shear Behavior between MICP-Treated Calcareous Sand and Steel.” *Journal of Materials in Civil Engineering*, 33(2), 04020455.

Lin, S., Lei, X., Meng, Q., and Xu, J. (2019). “Properties of biocemented, basalt-fibre-reinforced calcareous sand.” *Institute of Civil Engineers - Ground Improvement*.

Liu, L., Liu, H., Stuedlein, A. W., Evans, T. M., and Xiao, Y. (2019). “Strength, stiffness, and microstructure characteristics of biocemented calcareous sand.” *Canadian Geotechnical Journal*, 56(10), 1502–1513.

Liu, L., Liu, H., Xiao, Y., Chu, J., Xiao, P., and Wang, Y. (2018). “Biocementation of calcareous sand using soluble calcium derived from calcareous sand.” *Bulletin of Engineering Geology and the Environment*, 77(4), 1781–1791.

Miftah, A., Khodadadi Tirkolaei, H., and Bilsel, H. (2020). “Biocementation of Calcareous Beach Sand Using Enzymatic Calcium Carbonate Precipitation.” *Crystals*, 10(10), 888.

Mitchell, J. K., and Soga, K. (2005). *Fundamentals of Soil Behavior*. John Wiley & Sons, Hoboken.

Montoya, B., and DeJong, J. (2015). “Stress-Strain Behavior of Sands Cemented by Microbially Induced Calcite Precipitation.” *J. Geotech. Geoenviron. Eng.*, 10.

Montoya, B. M., DeJong, J. T., and Boulanger, R. W. (2013). “Dynamic response of liquefiable sand improved by microbial-induced calcite precipitation.” 63(4), 302–312.

Montoya, B. M., Gerhard, R., DeJong, J. T., Wilson, D. W., Weil, M. H., Martinez, B. C., and Pederson, L. (2012). “Fabrication, Operation, and Health Monitoring of Bender Elements for Aggressive Environments.” *Geotechnical Testing Journal*, 35(5), 103300.

Oualha, M., Bibi, S., Sulaiman, M., and Zouari, N. (2020). “Microbially induced calcite precipitation in calcareous soils by endogenous Bacillus cereus, at high pH and harsh weather.” *Journal of Environmental Management*, 257, 109965.

van Paassen, L. A. (2011). “Bio-Mediated Ground Improvement: From Laboratory Experiment to Pilot Applications.” *Geo-Frontiers 2011*, American Society of Civil Engineers, Dallas, Texas, United States, 4099–4108.

Raymond, A. J., Kendall, A., and DeJong, J. T. (2020). “Life Cycle Sustainability Assessment (LCSA): A Research Evaluation Tool for Emerging Geotechnologies.” *Geo-Congress 2020*, American Society of Civil Engineers, Minneapolis, Minnesota, 330–339.

San Pablo, A. C. M., Lee, M., Graddy, C. M. R., Kolbus, C. M., Khan, M., Zamani, A., Martin, N., Acuff, C., DeJong, J. T., Gomez, M. G., and Nelson, D. C. (2020). “Meter-Scale Biocementation Experiments to Advance Process Control and Reduce Impacts: Examining Spatial Control, Ammonium By-Product Removal, and Chemical Reductions.” *Journal of Geotechnical and Geoenvironmental Engineering*, 146(11), 04020125.

Stocks-Fischer, S., Galinat, J. K., and Bang, S. S. (1999). “Microbiological precipitation of CaCO3.” *Soil Biology and Biochemistry*, 31(11), 1563–1571.

U.S. Environmental Protection Agency. (2013). “Aquatic Life Ambient Water Quality Criteria for Ammonia – Freshwater.” *EPA Publication No. 822-R-13-001*, 1–255.

Wang, Y. -J., Han, X.-L., Jiang, N.-J., Wang, J., and Feng, J. (2021). “The effect of enrichment media on the stimulation of native ureolytic bacteria in calcareous sand.” *International Journal of Environmental Science and Technology*.

Wirth, X., Benkeser, D., Yeboah, N. N. N., Shearer, C. R., Kurtis, K. E., and Burns, S. E. (2019a). “Evaluation of Alternative Fly Ashes as Supplementary Cementitious Materials.” *ACI Materials Journal*, 116(4).

Wirth, X., Glatstein, D. A., and Burns, S. E. (2019b). “Mineral phases and carbon content in weathered fly ashes.” *Fuel*, 236, 1567–1576.

Xiao, P., Liu, H., Stuedlein, A. W., Evans, T. M., and Xiao, Y. (2019). “Effect of relative density and biocementation on cyclic response of calcareous sand.” *Canadian Geotechnical Journal*, 56, 1849–1862.

Xiao, P., Liu, H., Xiao, Y., Stuedlein, A. W., and Evans, T. M. (2018). “Liquefaction resistance of bio-cemented calcareous sand.” *Soil Dynamics and Earthquake Engineering*, 107, 9–19.